25

Ambrose, W. A., K. Fouad, S. Sakurai, D. C. Jennette, L. F. Brown Jr., E. H. Guevara, D. B. Dunlap, T. F. Wawrzyniec, S. C. Talukdar, M. A. Garcia, U. H. Romano, H. R. Ruiz, R. C. Hernández, J. A. Vega, and E. M. Zamora, 2009, Neogene tectonic, stratigraphic, and play framework of the southern Laguna Madre–Tuxpan continental shelf, Gulf of Mexico, *in* C. Bartolini and J. R. Román Ramos, eds., Petroleum systems in the southern Gulf of Mexico: AAPG Memoir 90, p. 477–502.

Neogene Tectonic, Stratigraphic, and Play Framework of the Southern Laguna Madre–Tuxpan Continental Shelf, Gulf of Mexico

William A. Ambrose, Khaled Fouad, Shinichi Sakurai, David C. Jennette, L. F. Brown Jr., Edgar H. Guevara, and Dallas B. Dunlap

Bureau of Economic Geology, John A. and Katherine G. Jackson School of Geosciences, the University of Texas at Austin, Austin, Texas

Tim F. Wawrzyniec

Department of Earth and Planetary Sciences, 1 University of New Mexico, Albuquerque, New Mexico

Suhas C. Talukdar

Consultant The Woodlands, Texas

Mario Aranda Garcia, Ulises Hernández Romano, Hector Ruiz Ruiz, and Ramón Cárdenas Hernández

Petroleos Mexicanos Exploración y Producción, Edificio de Exploración Int. Campo Pemex (Anexo al Activo de Prod. Poza Rica) Poza Rica, Veracruz, Mexico

Juan Alvarado Vega and Eduardo Macías Zamora

Petroleos Mexicanos Exploración y Producción, Tampico, Tamaulipas, Mexico

ABSTRACT

Neogene shelf, slope, canyon, and slope-to-basin-floor transition plays in the southern Laguna Madre–Tuxpan (LM-T) continental shelf reflect a variety of structural and stratigraphic controls, including gravity sliding and extension, compression, salt evacuation, and lowstand canyon and fan systems. The Neogene in the LM-T area was deposited along narrow shelves associated with a tectonically active coast affected by significant uplift and erosion of carbonate and volcanic terrains. This study characterizes 4 structurally defined trends and 32 Neogene plays in a more than 50,000-km^2 (19,300-mi^2) area linking the Veracruz and Burgos basins.

Reprinted from AAPG Bulletin, v. 89, no. 6, (June 2005), pp. 725–751.
DOI:10.1306/13191099M903340

The Cañonero trend in the southern part of the LM-T area contains deep-seated basement faults caused by Laramide compression. Many of these faults are directly linked to the interpreted Mesozoic source rocks, providing potential pathways for vertically migrating hydrocarbons. In contrast, the Lankahuasa trend, north of the Cañonero trend, contains listric faults, which detach into a shallow horizon. This trend is associated with thick Pliocene shelf depocenters. The dominant plays in the Faja de Oro–Náyade trend in the central part of the LM-T area contain thick lower and middle Miocene successions of steeply dipping slope deposits, reflecting significant uplift and erosion of the carbonate Tuxpan platform. These slope plays consist of narrow channel-fill and levee sandstones encased in siltstones and mudstones. Plays in the north end of the LM-T area, in the southern part of the Burgos basin, contain intensely deformed strata linked to salt and shale diapirism. Outer-shelf, slope, and proximal basin-floor plays in the Lamprea trend are internally complex and contain muddy debris-flow and slump deposits.

Risk factors and the relative importance of play elements vary greatly among LM-T plays. Reservoir quality is a critical limiting play element in many plays, especially those in the Cañonero trend directly downdip from the trans-Mexican volcanic belt, as well as carbonate-rich slope plays adjacent to the Tuxpan platform. In contrast, trap and source are low-risk play elements in the LM-T area because of the abundance of large three-way and four-way closures and the widespread distribution of organic-rich Upper Jurassic Tithonian-age source rock. The potential for hydrocarbon migration in LM-T plays is a function of the distribution of deep-seated faults inferred to intersect the primary Mesozoic source. Their distribution is problematic for the Lankahuasa trend, where listric faults sole out into the Paleocene. Seal is poorly documented for LM-T plays, although the presence of overpressured zones and thick bathyal shales is favorable for seal development in middle and lower Miocene basin and slope plays.

OBJECTIVE, DATABASE, AND METHODS

The objective of this study was to provide a geologic framework for defining and delineating Miocene and Pliocene gas plays in the southern Laguna Madre–Tuxpan (LM-T) continental shelf and adjacent onshore areas (Figure 1). The study was conducted jointly by the Bureau of Economic Geology and Petroleos Mexicanos Exploración y Producción.

The Neogene trend in the LM-T continental shelf is a frontier area for oil and gas exploration in the Gulf Coast. The only offshore Neogene discoveries at the time of this writing occur in upper Miocene shelf and lower Pliocene slope sandstones in the Lankahuasa trend. Production in the eastern Mexico continental shelf has historically been from Mesozoic carbonate reservoirs in the area of the Faja de Oro and Sardina three-dimensional (3-D) surveys (Figure 1). Although approximately 20 wells are present in the area of these two 3-D surveys, the Neogene section in most of these wells has neither been completely logged nor fully evaluated. Moreover, most of the 32 Neogene hydrocarbon plays defined and mapped in this study have yet to be fully tested with exploratory wells. This integrated geologic study delineates the major tectonic and structural features, maps the principal paleogeographic elements and facies tracts, and characterizes Neogene plays in terms of their principal play elements, including reservoir quality and presence, trap, seal, source, migration, and timing.

The study area encompasses more than 50,000 km^2 (19,300 mi^2) and includes the offshore continental shelf between the Veracruz and Burgos basins to the 500-m (1600-ft) isobath, plus a small part of onshore Mexico (Figure 1). The eastern limit of the study area encompasses the Neogene paleoshelf, slope, and slope-to-basin-floor transition, with abyssal plain areas lying east of the mapped area. The database consists of six 3-D seismic surveys, collectively covering more than 8000 km^2 (3088 mi^2), as well as more than 14,000 linear km of offshore and onshore two-dimensional (2-D) lines (not shown). Twenty-seven offshore and eighteen onshore wells are included in the study. Four offshore wells are in the Lankahuasa 3-D survey area, ten are within the area of the Faja de Oro 3-D survey, ten are in the Sardina 3-D survey area, two are inside the Náyade 3-D survey area, and one is in the Lamprea 3-D survey area. Twelve

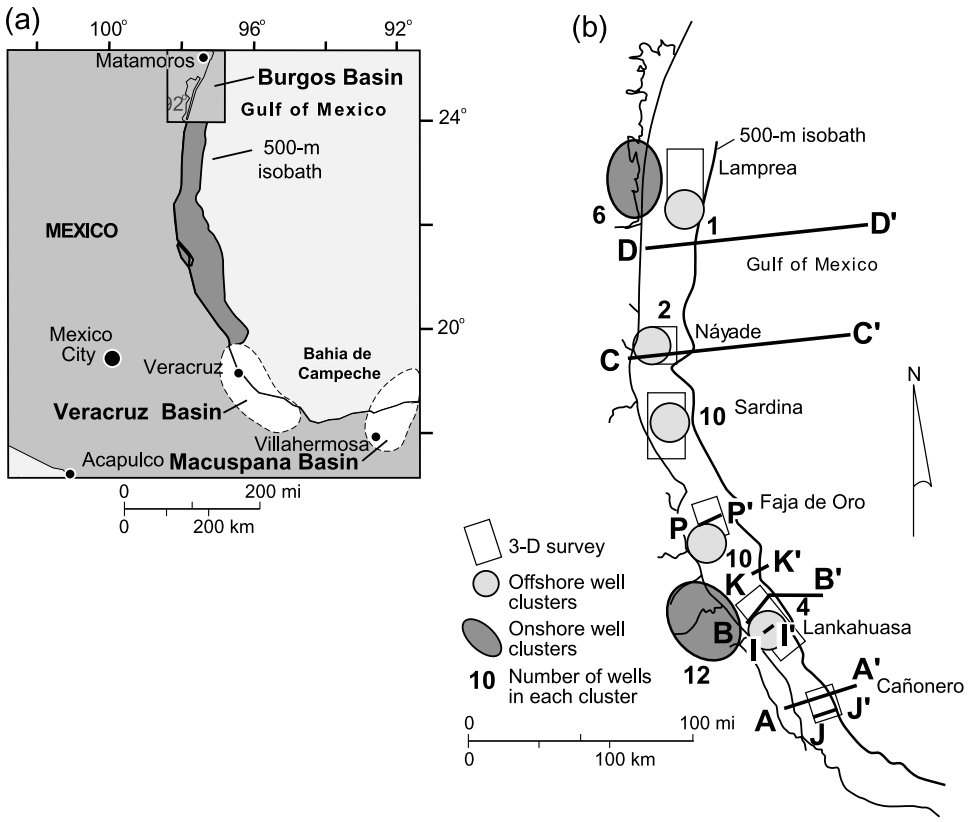

FIGURE 1. (a) Location of the southern LM-T continental shelf and adjacent Veracruz and Burgos basins. (b) Distribution of 3-D seismic surveys used in this study. Seismic sections AA′ to DD′ are shown in Figure 4. Seismic section II′ is shown in Figure 7a. Seismic section JJ′ is shown in Figure 7b. Seismic section KK′ is shown in Figure 8. Seismic section PP′ is shown in Figure 9b.

onshore wells that occur in clusters penetrate the middle Miocene, and deeper sections are west of the Lankahuasa 3-D survey. Six onshore wells are from onshore areas west of the Lamprea 3-D survey (Figure 1b). Of these onshore wells, approximately one-half contain usable logs and information from cuttings.

The study area was divided into four structural trends (Cañonero, Lankahuasa, Faja de Oro–Náyade, and Lamprea [Figure 2]). Each trend, described in more detail in the section on structural framework, was delineated on the basis of variations in timing and style of structural elements and served as a framework for evaluating trap, migration, and timing for each play.

The tops of the Mesozoic (structural basement) and regional detachments were mapped to document the structural elevation of inferred Mesozoic potential source rocks and to highlight areas of greater fault connectivity to this interpreted source interval. Mapped closures were evaluated from structure maps to define trap styles and to quantify trap density.

The Neogene section was divided into eight principal stratigraphic units bounded by regional unconformities, flooding, and fan-abandonment surfaces, which, from oldest to youngest, are (1) lower Miocene_1, (2) lower Miocene_2, (3) middle Miocene, (4) upper Miocene_1, (5) upper Miocene_2, (6) lower Pliocene, (7) middle Pliocene, and (8) upper Pliocene (Figure 3). Many of the regional stratal surfaces in the LM-T area were extrapolated from those recognized and correlated in the Bureau of Economic Geology–Petroleos Mexicanos regional study of the adjacent Veracruz basin (Jennette et al., 2003). An informal, two-part stratigraphic nomenclature scheme used for the Miocene section in this study (for example, FS40 and SB43) was adopted from Jennette et al. (2003). Biostratigraphic data from both onshore and offshore wells were used to constrain the age and paleobathymetry of flooding surfaces and fan-abandonment surfaces. The age of intervals defined in the study was determined in studies of foraminifera and nannoplankton assemblages conducted by paleontologists at the Petroleos Mexicanos and Instituto Mexicano del Petróleo.

Petrophysical models were constructed for wells with the best rock and log data. The latter typically consisted of gamma-ray, resistivity, density, sonic, and neutron curves. These models provided computations of water saturation (S_w), shale volume (V_{sh}), porosity (ϕ), and net pay (oil- or gas-bearing reservoir), parameters used in assessing reservoir quality and reservoir presence.

A geochemical study was conducted to define the source of known oil and gas occurrences, to identify oil- and gas-generating source rocks and recognize their relative importance, to define hydrocarbon-generating areas and timing of oil and gas generation and migration from different source rocks, and to infer which hydrocarbon types may be available for Neogene plays in different parts of the study area and evaluate the risk

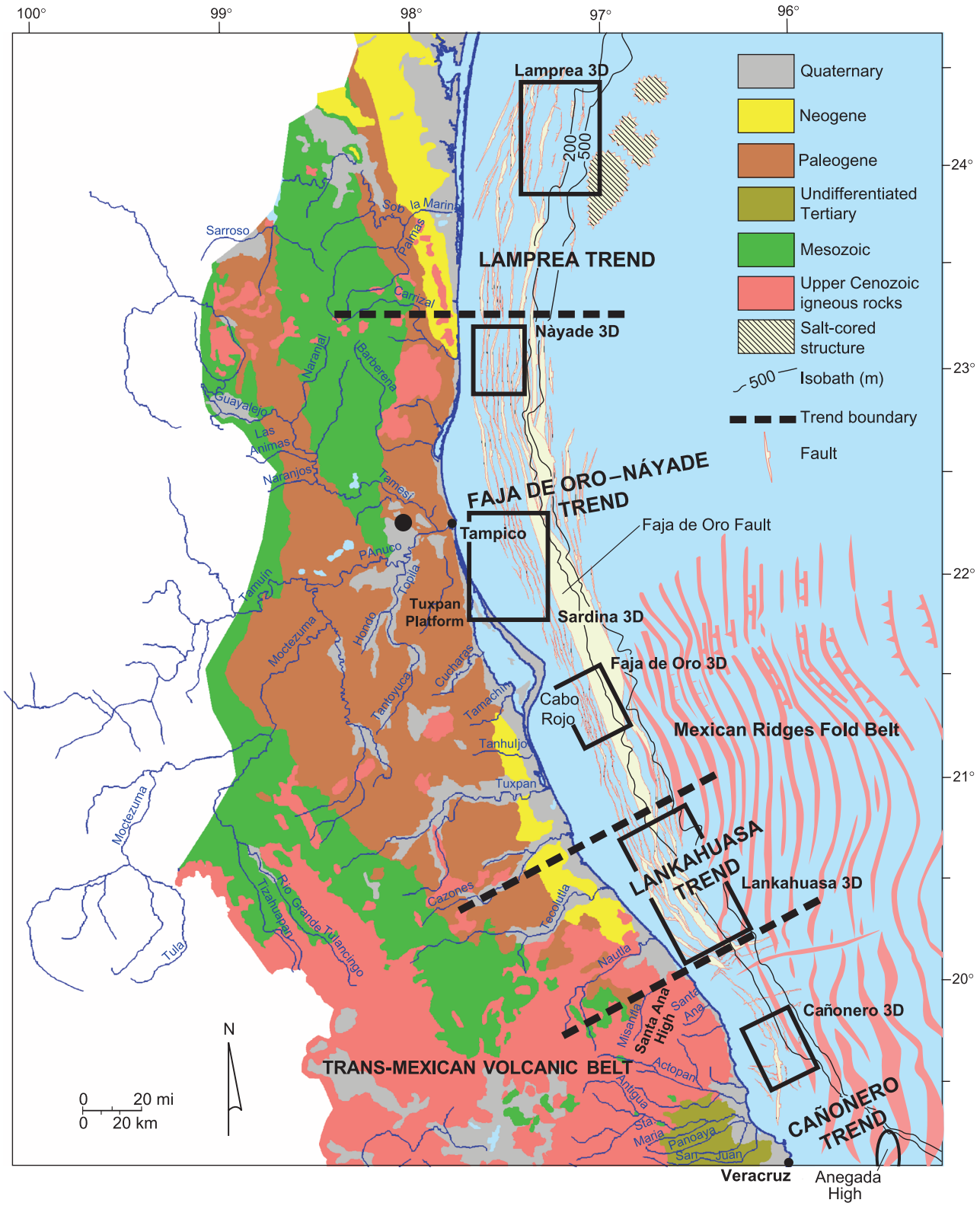

FIGURE 2. Physiographic provinces, structural trends, and 3-D seismic surveys in the southern LM-T continental shelf and adjacent areas.

factors for hydrocarbon charge. The geochemistry database included total organic carbon (TOC) and pyrolysis data on source rocks, vitrinite reflectance (R_o) data, gas-composition data, carbon-isotope data from sea-bottom sediment cores, bottomhole-temperature data, and heat-flow data from eight offshore locations. Data on gases,

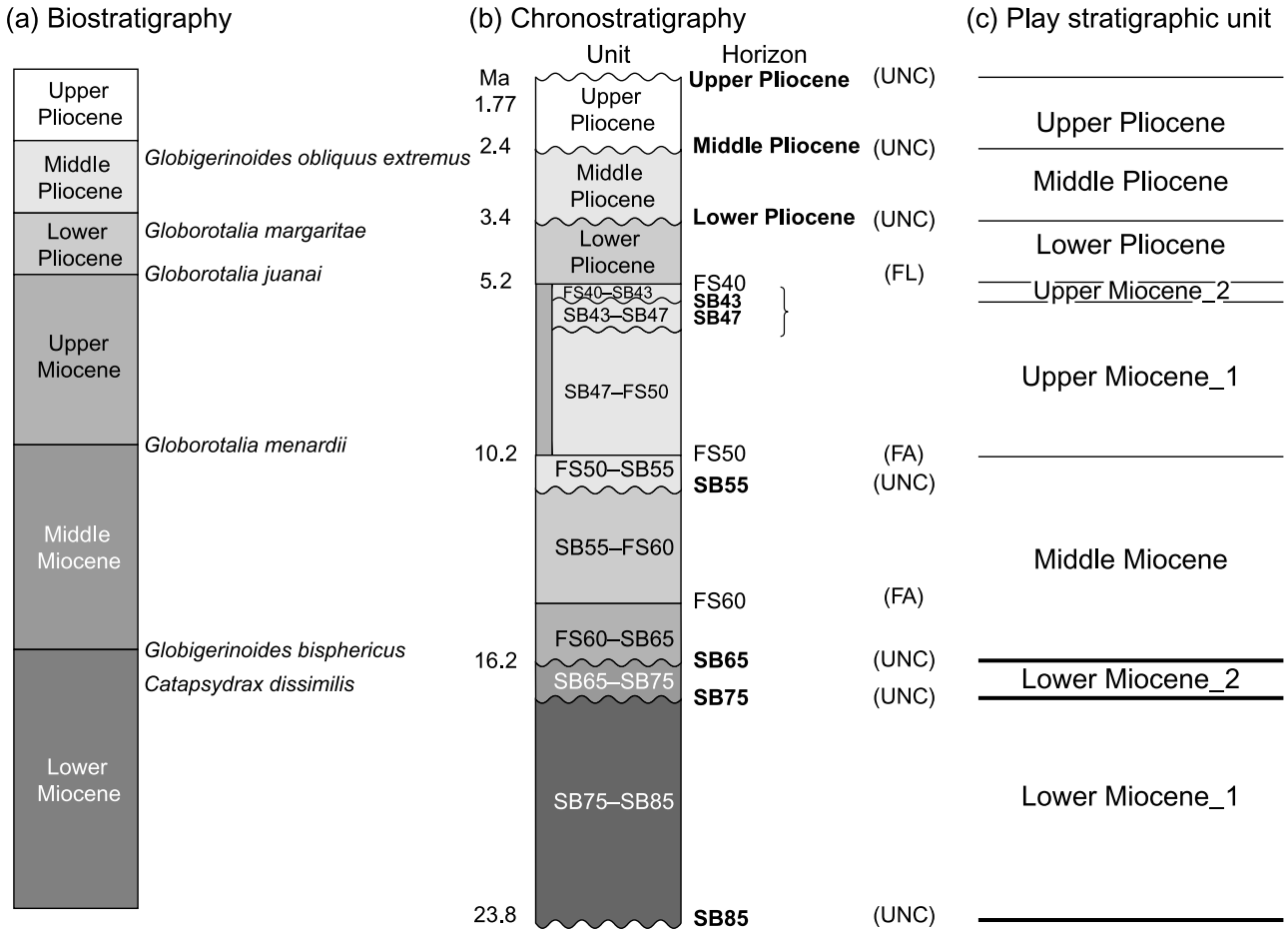

FIGURE 3. Laguna Madre–Tuxpan Neogene stratigraphic columns. (a) Major biostratigraphic horizons. (b) Chronostratigraphy and informal stratigraphic units correlated and mapped in this study, with stratigraphic occurrence of major sequence boundaries (unconformities) and flooding surfaces. (c) Play stratigraphic units defined and mapped in this study. Abbreviations: UNC = unconformity; FL and FS = flooding surface; FA = fan-abandonment surface; SB = sequence boundary. Biostratigraphic nomenclature and ages are based on Petroleos Mexicanos data.

oils, and source rocks were also used for interpretation, and other data were available from Mello et al. (1996), Román-Ramos et al. (1996), Guzmán-Vega and Mello (1999), Goldhammer and Johnson (2001), González and Holguín (2001), Guzmán-Vega et al. (2001), Magoon et al. (2001), Román-Ramos and Holguín-Quiñones (2001), and Jordan and Wilson (2003).

The 32 Neogene plays were defined using a two-stage classification scheme, consisting of (1) geologic age, with eight divisions in the Miocene and Pliocene, and (2) principal paleogeographic type, including shelf, slope, slope-to-basin-floor transition, and channelized facies composed of submarine-canyon deposits. Paleogeographic types were inferred from geometry and character of seismic reflectors in regional dip lines, supplemented with core and log data, as well as from isochron and amplitude-extraction maps. Isochron maps were particularly effective in delineating the regional distribution of basin-floor fans, where a strong relation was inferred to exist between fan depocenters and interval thickness.

Plays were characterized using a variety of play elements, including reservoir presence and quality, trap, seal, source, migration, and timing. Criteria were established for assessing play elements for each play. For example, reservoir quality was inferred directly from core and petrographic data and indirectly from log computations. For those play elements for which data were sparse or absent in the study area, analogs from adjacent and nearby basins in the Gulf Coast were used. Criteria for all play elements evaluated in this study are described in the section on plays. Play ranking is not addressed in this paper, as results are confidential. However, general comments are provided for the relative adequacy of each major play element for LM-T plays (see Table 1 and the section on play elements).

Table 1. Play-element adequacy for the Laguna Madre–Tuxpan plays in the Cañonero, Lankahuasa, Faja de Oro–Náyade trends.*

Trend	*Play*	*Reservoir Presence and Quality*	*Trap*	*Seal*	*Source*	*Timing and Migration*
Cañonero	shelf	untested	untested	untested	*favorable*	*favorable*
	slope	untested	untested	*favorable*	*favorable*	*favorable*
	slope-to-basin-floor transition	*unfavorable*	favorable	*favorable*	*favorable*	*favorable*
	canyon	unfavorable	favorable	*favorable*	*favorable*	*favorable*
Lankahuasa	shelf	proven	proven	proven	proven	proven
	slope	proven	proven	proven	proven	proven
	slope-to-basin-floor transition	*favorable*	favorable	*favorable*	*favorable*	untested
	canyon	*unfavorable*	untested	*favorable*	*favorable*	*favorable*
Faja de Oro–Náyade	shelf	untested	*unfavorable*	untested	*favorable*	untested
	slope	proven	proven	proven	proven	proven
	slope-to-basin-floor transition	*favorable*	favorable	*favorable*	*favorable*	untested
	canyon	untested	untested	untested	*favorable*	untested
Lamprea	shelf	favorable	*favorable*	untested	*favorable*	*favorable*
	slope	unfavorable	*unfavorable*	unfavorable	*favorable*	untested
	slope-to-basin-floor transition	untested	favorable	untested	*favorable*	untested
	canyon	untested	untested	untested	*favorable*	untested

**Proven = plays with established production or favorable production tests. Favorable = production not yet established, but existing data indicate adequacy. Unfavorable = production not yet established, and existing data suggest inadequacy. Untested = production not yet established, and insufficient data exist to evaluate adequacy. Italics = production not established, and although insufficient play-element data are present, adequacy is inferred from facies and play analogs from the neighboring Veracruz and Burgos basins. Data types and criteria indicating adequacy are discussed in the text section Play Elements.*

STRUCTURAL FRAMEWORK

Regional Tectonic Setting

The LM-T continental shelf was initially established as a series of sediment-starved, Jurassic carbonate platforms that formed on a relatively thick, extended, and modified continental crust (Feng et al., 1994). Pindell (1994) and Pindell et al. (2000) associated this modified crust with back-arc, south-southeast–directed extension and the opening of the Areperos Ocean, which is thought to be a back-arc extension related to the northwest-directed compression along the west coast of North America. Alternatively, others contended that the extended crust of the early LM-T shelf represents an attenuated crust directly associated with the south-southeast–directed opening of the Gulf of Mexico (Buffler, 1983; Buffler and Sawyer, 1985; Marton and Buffler, 1994; Wawrzyniec et al., 2003).

Following the opening of the Gulf of Mexico, the early, western shelf of the Gulf was a relatively stable, clastic-sediment-starved, carbonate platform (Buffler, 1983; Watkins and Buffler, 1996). The first major influx of siliciclastic sediment on the shelf occurred during the Paleocene. The onset of the Sevier-Laramide orogeny resulted in differential landward uplift and subsidence of the Cretaceous Tuxpan carbonate platform (Winker, 1984; Galloway et al., 2000). By the late Paleocene to early Eocene, the shelf was dominated largely by erosion and sediment bypass. However, by the end of the Eocene, fluvial-dominated deltas prograded eastward, a consequence of increased sediment supply and uplift in the Sevier-Laramide hinterland. By the Oligocene, the Tuxpan platform was buried by siliciclastic sediments. Throughout the Neogene and Quaternary, the shelf was dominated by siliciclastic deposits, recording a complex interplay between tectonic uplift, subsidence, and eustasy.

Structures recognized in the LM-T shelf include multiple east-dipping, synthetic faults that sole into a single detachment (Feng et al., 1994; Trudgill et al., 1999) and associated hanging-wall monoclines. These structures are the direct result of depositional loading and subsequent basinward gravitational sliding of strata (Buffler, 1983). Extensional grabens along the shelf were mechanically linked to compression in the Mexican

Ridges fold belt (Figure 2) and gravitational gliding along a weak detachment horizon in the shaly Oligocene section (Buffler, 1983; Feng et al., 1994; Trudgill et al., 1999; Wawrzyniec et al., 2003).

Local Structural Trends and Physiographic Setting

The LM-T area is divided from south to north into four structural trends: the Cañonero, Lankahuasa, Faja de Oro–Náyade, and Lamprea (Figure 2). Each trend is delineated on the basis of variations in timing and style of structural elements. Other important physiographic elements and structural features include the trans-Mexican volcanic belt, Santa Ana high, Mexican Ridges fold belt, and Tuxpan platform (Figure 2).

The trans-Mexican volcanic belt is related to subduction along the Mid-American trench and is about 200 km (124 mi) from the boundary between the Cocos and North American plates (Pindell, 1994; Ferrari et al., 1999). Volcanism in the Cañonero and southern part of the Lankahuasa trends is recorded seismically in the form of bright-amplitude, high-impedance middle and upper Miocene intrusive bodies and tuffaceous debris-flow deposits. The Santa Ana high is a basement uplift located in the trans-Mexican volcanic belt. It is also associated with a basinward deflection of basement structures and serves as the southern boundary of the growth-fault-dominated Lankahuasa trend (Figure 2). The Mexican Ridges fold belt, extending from the north end of the Veracruz basin to the deep offshore, more than 150 km (93 mi) east of Cabo Rojo, is a series of subparallel, north- and northwest-trending folds related to downdip compression and shortening at the distal end of major detachment faults (Pew, 1982) (Figure 2). The Tuxpan platform, located south of Tampico, is a Cretaceous carbonate platform that forms the western boundary of the Faja de Oro fault system. This fault system commonly offsets lower Miocene strata by hundreds of meters.

Cañonero Trend

The Cañonero trend, located downdip (eastward) of the trans-Mexican volcanic belt, is the northern continuation of the Veracruz basin. It contains deep-seated basement faults associated with compression and strike-slip motion. Strike-slip trends along the Anegada high continue along strike until they terminate along the east end of the Santa Ana high. Growth in Neogene strata along major east-dipping faults is relatively minor in lower and middle Miocene strata and more significant in upper Miocene and Pliocene strata in the Cañonero trend (Figure 4a). Anticlinal structures east of these main east-dipping faults in the Cañonero trend commonly contain four-way closures associated with middle Miocene to Pliocene inversion. Middle Miocene folds in the Cañonero trend may have had a bathymetric expression because they coincide with the basinward limit of many lower to middle Miocene lowstand basin-floor-fan complexes. The folds appear to have been initiated at the same time, with the more eastward folds continuing to actively deform to the present day. This deformation is evident in the bathymetric expression of normal faults that appear to accommodate crestal collapse of these roughly coast-parallel folds.

Lankahuasa Trend

The Lankahuasa trend is dominated by gravity-sliding tectonics and extensional grabens, where most of the fault displacement is accommodated in the Pliocene strata (Figure 4b). The major faults in the Lankahuasa trend are a series of shallow-detachment listric faults associated with shelf depocenters of upper Miocene and Pliocene age. The Lankahuasa trend contains numerous synthetic faults associated with primary or multiple antithetic faults, all of which appear to be synkinematic throughout the Neogene. The result was the formation of multiple wine-glass-shaped extensional grabens that grew younger and more developed basinward. Where these grabens are positioned over basement highs, strata in them form rollover structures. These grabens are associated with numerous, small-scale, three-way closures and areally limited, fault-bounded, low-impedance amplitude anomalies.

Faja de Oro–Náyade Trend

The Faja de Oro–Náyade trend, north of the Lankahuasa trend, occurs where several large listric faults take a basinward step and merge into a primary synthetic listric fault (Faja de Oro fault) that extends along the coast for nearly 200 km (124 mi). Updip of this fault is a system of synthetic, listric faults whose offset appears to have been arrested at the time that the main fault formed (Figures 2, 4c). The net result is a series of synthetic normal faults that merge into a single detachment, with the most basinward fault having a pronounced rollover, hanging-wall fold, and net horizontal offset of 12–22 km (7.5–13.6 mi). The primary detachment appears to extend as a continuous subhorizontal plane that can be subdivided into two segments. The shallow segment overlies the buried carbonate shelf and occurs at a depth of 2–3 s (two-way traveltime [TWT]), directly below the base of the Miocene section. This segment terminates at the east edge of the platform, where it steps down into the deeper part of the basin. The deep part of the detachment is thought to be located at the top of regional geopressure, which is interpreted to lie within upper Cretaceous or lower Tertiary shales (Watkins and Buffler, 1996).

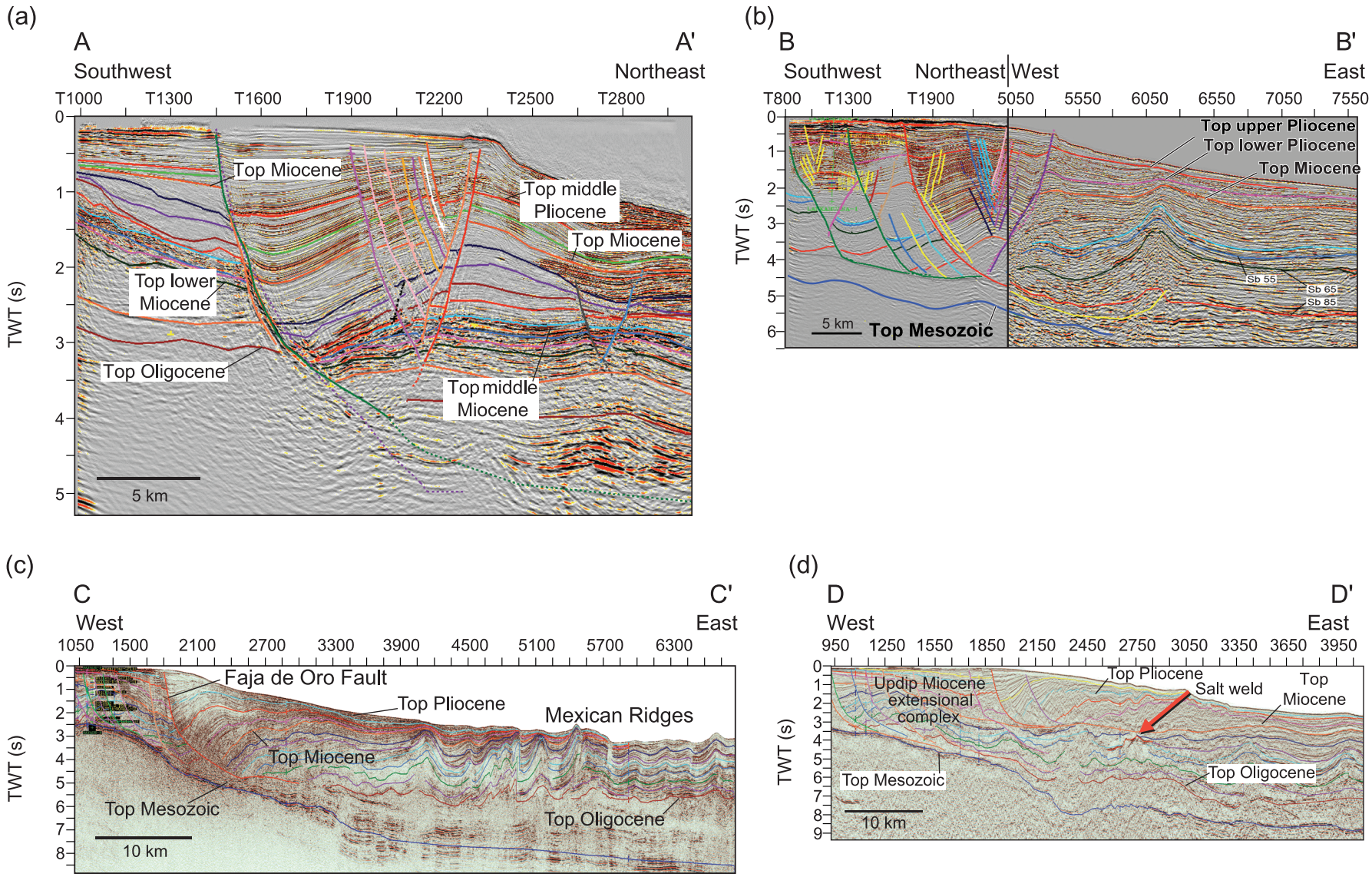

FIGURE 4. Seismic cross sections from the LM-T area. (a) Three-dimensional line AA′ from the south part of the Cañonero trend showing deeply penetrating, east-dipping master fault, associated with complex antithetic fault system. Vertical scale is TWT (ms). (b) Composite 3-D and 2-D line BB′ from the central part of the Lankahuasa trend showing highly extended Neogene section. (c) Two-dimensional line CC′ from the northern part of the Faja de Oro–Náyade trend, showing compressional Mexican Ridges fold belt. Vertical scale is TWT (ms). (d) Two-dimensional line DD′ from the Lamprea trend, illustrating an updip, upper Miocene extensional complex, a thick Pliocene section associated with growth faults, and salt welds. Vertical scale is TWT (seconds). Lines of section are shown in Figure 1.

Lamprea Trend

The southern boundary of the Lamprea trend is defined where greatly deformed strata are associated with salt and shale diapirism and salt withdrawal. The Lamprea trend is transitional northward to the Burgos basin (Figure 4d). This area contains Pliocene minibasins and slope-derived slump and debris-flow deposits, commonly developed above upper Miocene age salt welds. At least two distinct detachment levels are associated with structural styles consistent with halokinetic processes (Figure 4d). An updip Miocene extensional complex lies above the Cretaceous carbonate shelf and consists of synthetic, listric faults that sole into a detachment in the upper Paleocene section. This detachment appears to continue into the deep basin. However, a bright reflection at about 3.5 s TWT, located in the middle of the line, is interpreted to be a salt weld or a collapsed salt diapir. Furthermore, the position of this feature below a fault-bend-fold complex that modifies a lower Pliocene basin-floor-fan depocenter indicates that the salt extruded from this weld has since been displaced by the collapse of upper Pliocene inner slope depocenters. The second detachment became active in the lower Pliocene and soles into the base of the Pliocene, indicating that extension and gravitational collapse began as soon as the lower Pliocene strata began to blanket the extruded salt.

STRATIGRAPHIC FRAMEWORK

Unconformities

Sequences in the LM-T area are bounded by unconformities and defined in the manner described by Van Wagoner et al. (1990). Although some of these unconformities occur during periods of major eustatic sea level fall (Haq et al., 1987; Vail, 1987), in the LM-T area, they are thought to have been greatly influenced by local tectonic activity along the Sierra Madre Oriental orogenic belt. For example, the Veracruz basin, structurally continuous with the southern part of the LM-T area (Cañonero trend), was tectonically active throughout much of the Neogene, and major unconformities in this basin were produced through intermittent uplift along the Sierra Madre Oriental mountain belt (Jennette et al., 2002, 2003). Uplift in the western margin of the Veracruz basin resulted in major incision along a narrow shelf and delivery of large volumes of sediment to the basin floor. These deposits commonly directly overlie major unconformities and typically consist of submarine-canyon, channelized-fan, and sandy to conglomeratic basin-floor-fan facies.

Unconformities in LM-T area are inferred in seismic sections where there are abrupt, erosional contacts between units of different geometry and amplitude character. In the western (updip) part of the LM-T area, these unconformities are interpreted to be bypass surfaces associated with deep incision and canyons having hundreds of meters of erosional relief (Ambrose et al., 2003a) (Figure 5a). These canyons are interpreted to be 3–5 km (1.8–3.1 mi) wide, merging downdip (eastward) into a single, large canyon projected to the east edge of the Cañonero survey (Figures 5b, 6a). The canyon, varying in width from 5 to 8 km (3.1 to 5 mi), occurs as a single lenticular feature in strike section, associated with 400–550 ms (480–660 m; 1574–2165 ft) of erosion. The canyon-fill facies are differentiated into proximal- and distal-fill types (Figure 5b, c). The proximal canyon fill is defined by a relatively narrow (<5-km; <3.1-mi), asymmetrical strike profile, with a thick (>500-ms [>600-m; >1968-ft]) succession of nearly flat-lying, moderately bright-amplitude reflectors that lap onto the third-order basal SB43 unconformity (Figure 5b). In contrast, the distal canyon fill has a greater width-to-depth ratio and is more symmetrical in strike profile (Figure 5c). Downdip of the canyon system, the SB43 unconformity is nearly concordant with underlying reflectors and underlies a thick, bright-amplitude succession of basin-floor-fan deposits (Figure 5d).

Flooding and Fan-Abandonment Surfaces

Neogene flooding surfaces and fan-abandonment surfaces in the LM-T area commonly consist of dim amplitudes that form the upper bounding surface of sandy, bright-amplitude intervals (Figure 7). Flooding surfaces in the upper Miocene_2 (FS40 to SB43) interval in the Lankahuasa 3-D survey occur within thin (commonly <100-m [<330-ft]), dim-amplitude sections (Figure 7a). Two bright-amplitude successions in the upper Miocene_2 interval directly overlie sequence boundaries SB41 and SB43, respectively. These unconformities exhibit minor relief on the shelf. For example, the SB43 unconformity has virtually no detectable erosional relief in the western part of the Lankahuasa 3-D survey, and the SB41 unconformity is expressed in seismic lines as a bright-amplitude reflector having 10–25 ms (15–35 m; 49–114 ft) of relief, representing limited incision of valley-fill systems on the shelf (Figure 7a).

Fan-abandonment surfaces are also key stratigraphic horizons in the LM-T area, particularly those associated with thick, bright-amplitude lower and middle Miocene successions. For example, the fan-abandonment surface at the top of the middle Miocene (FS50) occurs at the base of a thick (>500-ms TWT [>600-m; >1968-ft]) section of dim-amplitude, muddy slope deposits (Figure 7b) and represents a regional chronostratigraphic surface, as well as a regionally extensive, potential seal above the middle Miocene section.

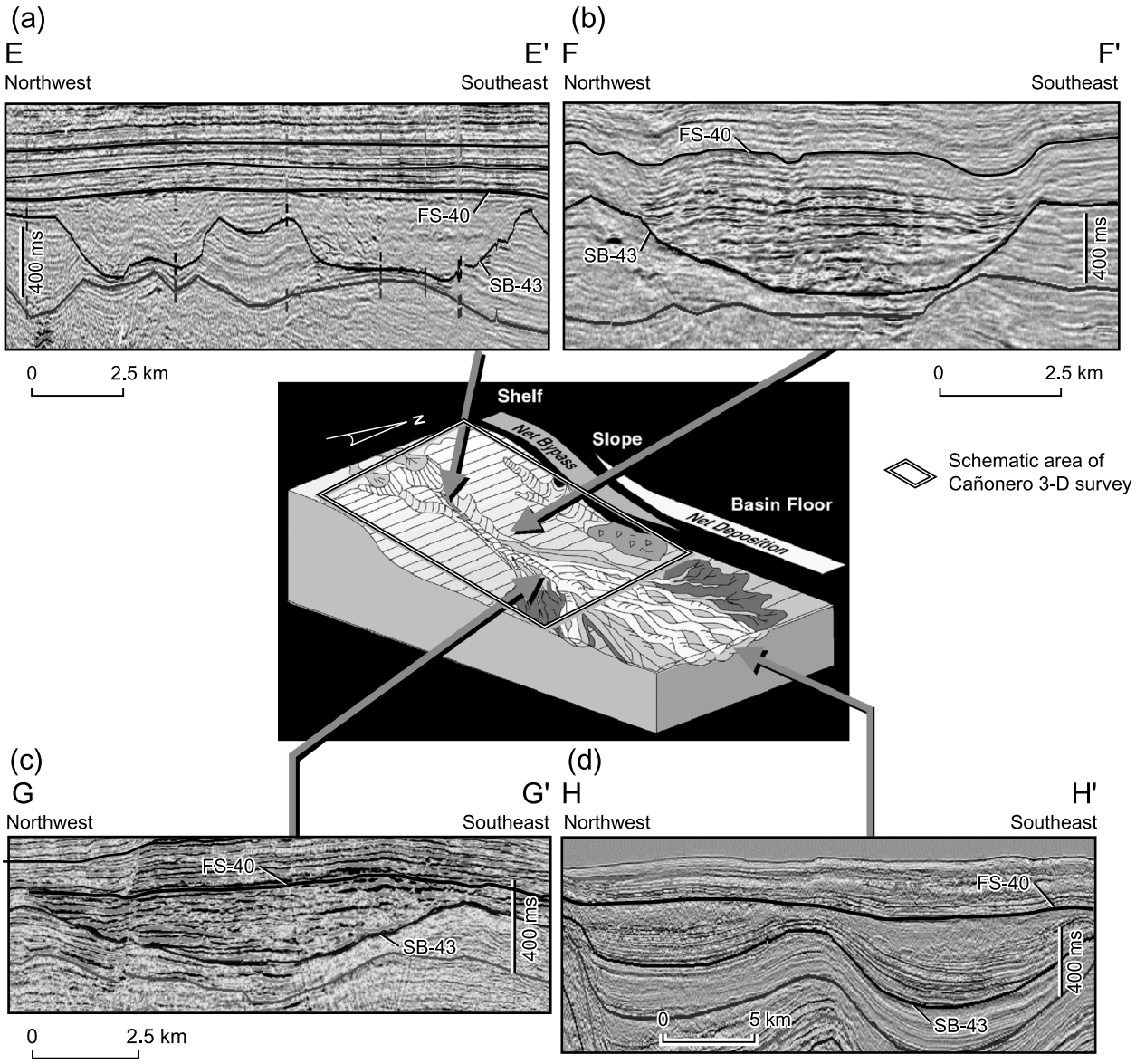

FIGURE 5. Schematic lowstand model depicting incised-slope, proximal-submarine-canyon, distal-submarine-canyon, and basin-floor-fan depositional systems, with cross-sectional insets providing examples from the upper Miocene_2 in the Cañonero trend. (a) EE′, dim-amplitude, shale-filled incised slope. (b) FF′, proximal-canyon fill. (c) GG′, distal-canyon fill. (d) HH′, basin-floor fan. Locations of sections (a–c) are shown in Figure 6a. Section (d) is approximately 10 km (6 mi) east of the Cañonero 3-D survey, and its location is shown in Figure 6b. Model modified from Beaubouef et al. (1999).

Paleogeography

Seismic-based paleogeographic maps, supplemented by log and core data, provide the foundation for defining and mapping LM-T plays. These maps are based on regional systematic changes in the geometry and amplitude character of reflectors observed in seismic sections (Figure 8).

Shelf seismic facies in this study are defined as sets of parallel reflectors updip (westward) of clinoforms. Although the overall geometry of reflectors in the shelf seismic facies is parallel, some individual reflectors are wavy and subparallel and are interpreted to represent small-scale valley fills notched into the shelf.

Slope seismic facies consist of clinoforms. The internal architecture of the slope facies is typically complex, with downlaps indicating prograding wedges and multiple erosional surfaces marking the bases of lowstand systems tracts.

Slope-to-basin-floor transition seismic facies are subdivided into two types, proximal and distal. The proximal facies are composed of wavy, subparallel sets of reflectors with moderate to bright amplitudes. These

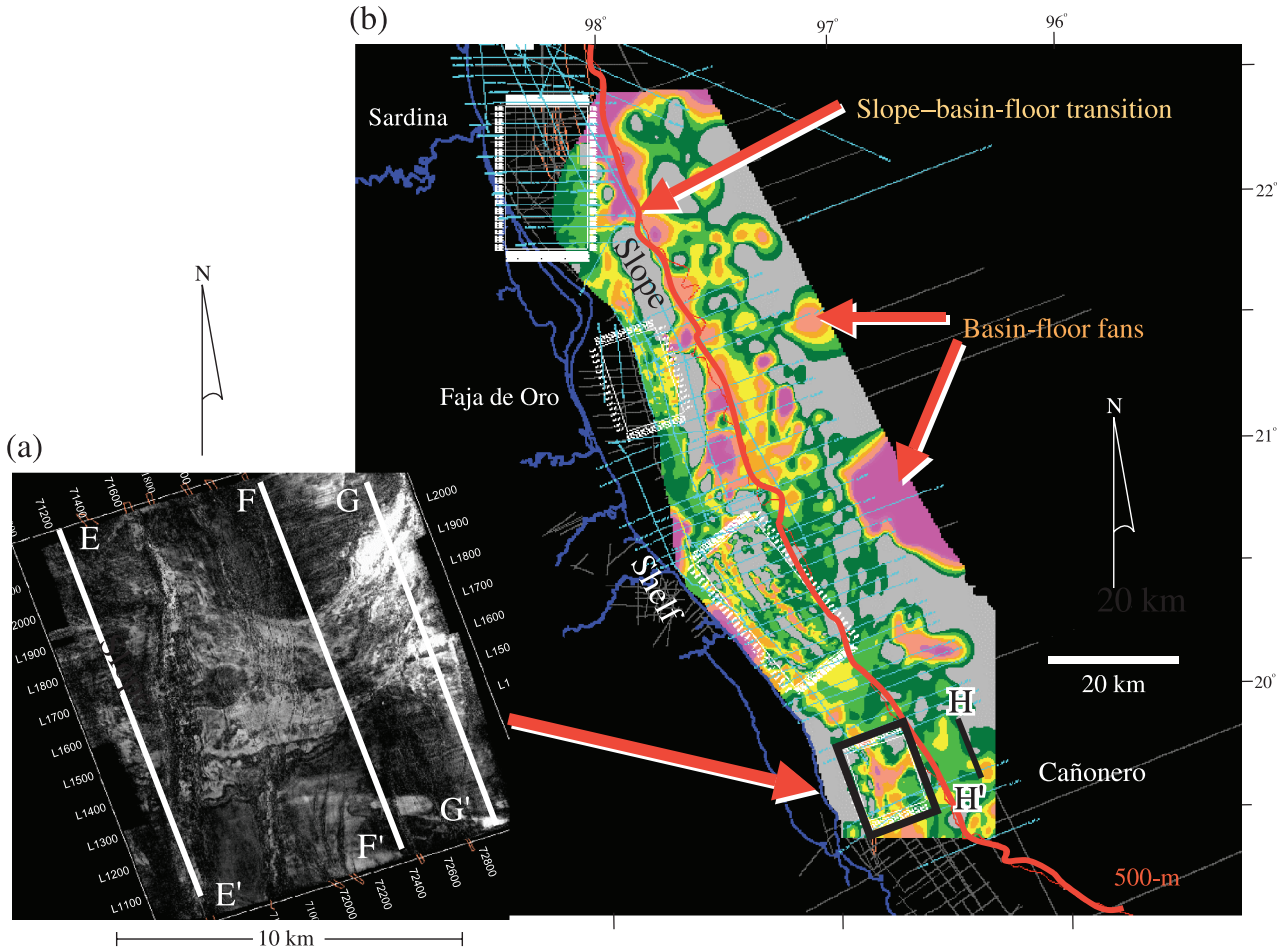

FIGURE 6. Upper Miocene_2 canyon systems. (a) Reflection-coefficient attribute map in the Cañonero 3-D survey, illustrating updip canyons merging eastward into a single, wider canyon. (b) Upper Miocene_2 isochron map, displaying regional context of the Cañonero canyon system. Large-scale, lobate, thick isochron features in the deep offshore (>500-m [>1600-ft] isobath) are interpreted to be basin-floor fans. Sections EE′ to HH′ are shown in Figure 5.

amplitudes in the Cañonero trend may represent thick accumulations of sandstone and/or conglomeratic sandstone, which are similar in seismic response to that of sandy and conglomeratic fan deposits in the adjacent Veracruz basin (Jennette et al., 2003). However, interpretation of recent data from similar deposits in the southern part of the Lankahuasa 3-D survey indicates the presence of volcanogenic conglomerates. Distal slope-to-basin-floor transition seismic facies are composed of parallel, dim-amplitude reflectors. Although the distal basin-floor seismic facies is composed of relatively dim amplitudes with respect to the proximal basin-floor facies, it may also be locally sandy, typically containing one or more thin zones of bright-amplitude reflectors.

The canyon seismic facies are interpreted to be major incision features. They are inferred from truncation of older reflectors by units with a lenticular cross-sectional geometry in strike view (Figure 5a–c) and are typically narrow and dip elongate in geometry (Figure 6a).

The Neogene in the LM-T area is an overall progradational, offlapping succession (Figures 9–11). The lower Miocene_1 (SB 75 to SB85) shelf edge is inferred to be west (onshore) of the modern Gulf of Mexico shoreline, and the slope-to-basin-floor transition is interpreted to be along the modern shoreline between the Lamprea and Sardina 3-D surveys (Figure 9a). The lower Miocene_1 slope in the Faja de Oro 3-D survey is a thick succession of steeply dipping wedges and clinoforms (Figure 9b). This section typically contains thin sandstones deposited in narrow, slightly sinuous, and dip-elongate channel and levee complexes (Figure 9c). These channel complexes are 1–2 km (0.6–1.2 mi) wide and are composed of amalgamated and multistoried channel complexes (commonly 10–30 m [33–100 ft] thick, interpreted from well data) and are associated with thin overbank sandstones.

The upper Miocene_2 (FS40 to SB43) shelf edge advanced eastward to the modern offshore (Figure 10a). In the central part of the Lamprea 3-D survey, the upper Miocene_2 stratigraphic unit is composed of high-impedance, slope mudstones (Figure 10b). Upper Miocene_2 cyclic shelf deposits (Figure 7a) are widely distributed in the western part of the Lankahuasa 3-D survey (Figure 10c).

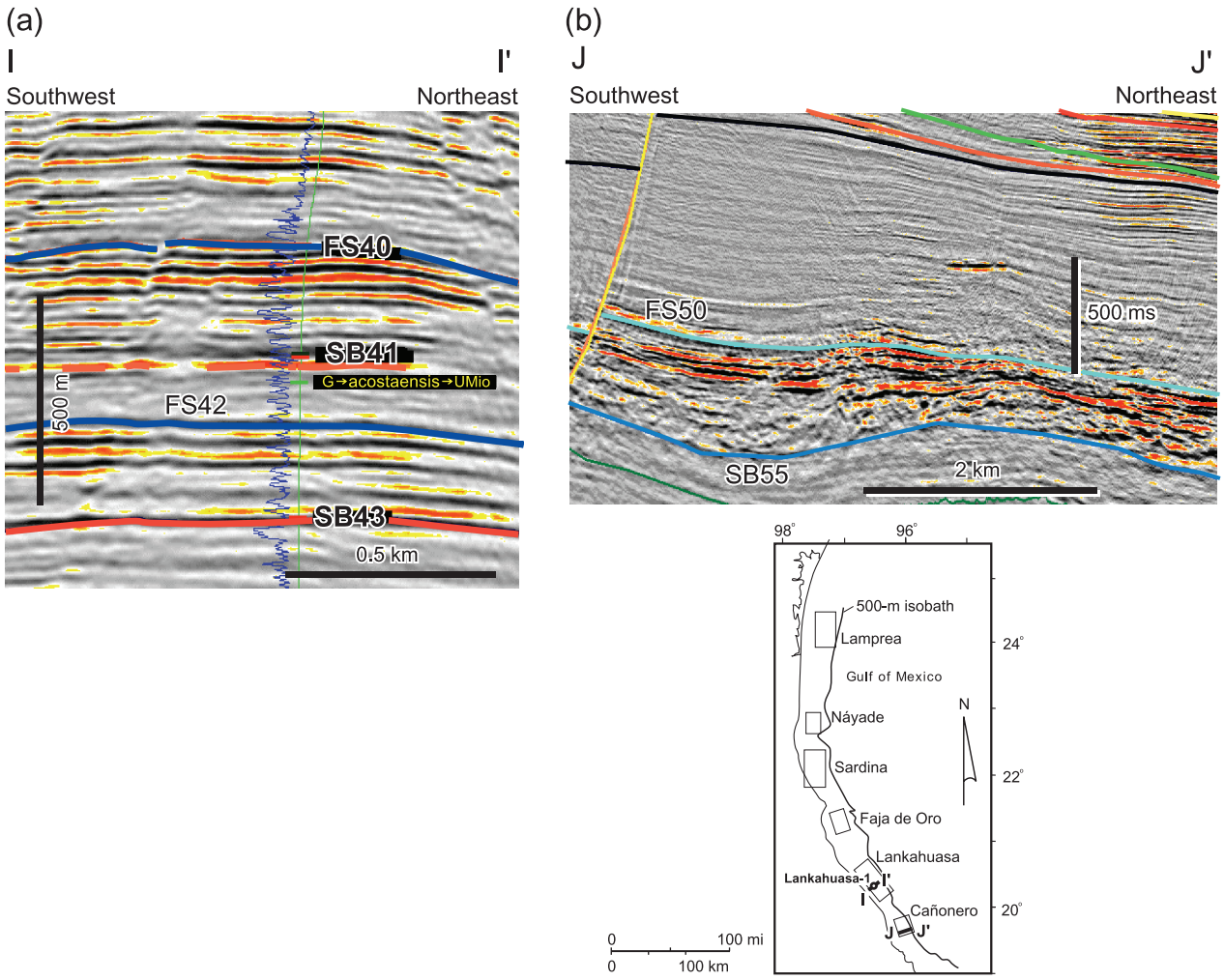

FIGURE 7. (a) Seismic section II′, showing log and seismic response of sequence boundaries (SB41, SB43) and flooding surfaces (FS40, FS42) in upper Miocene_2 shelf successions in the Lankahuasa-1 well. (b) Seismic dip section JJ′ in the Cañonero 3-D survey, showing seismic character of major fan-abandonment surface (FS50) at the top of the middle Miocene in the Cañonero 3-D survey. The Pemex 1 Lankahuasa is located in Figure 12. Cross section II′ is located in Figures 1 and 12a. Cross section JJ′ is located in Figure 1.

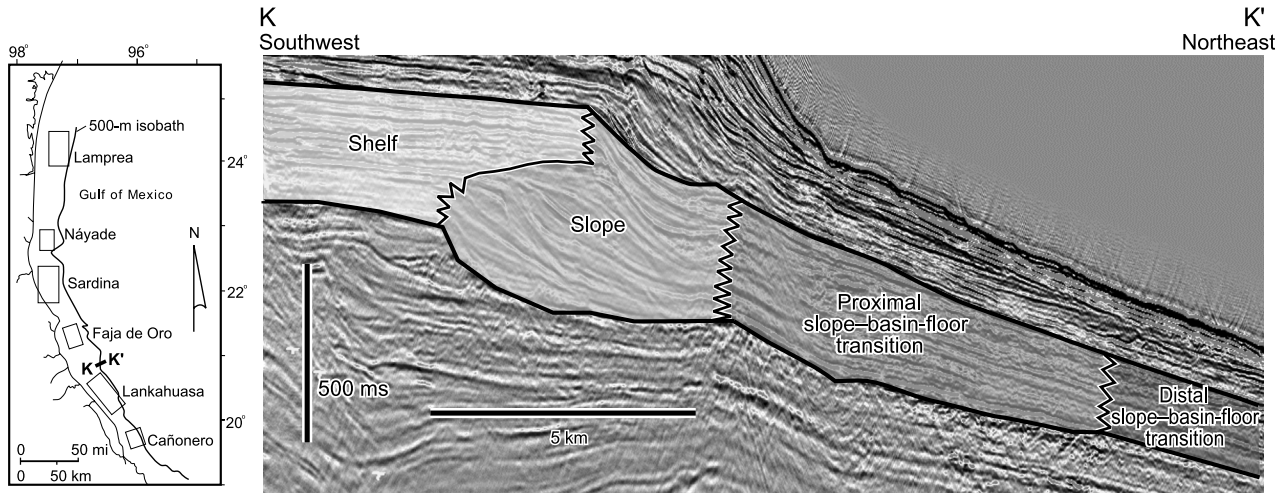

FIGURE 8. Two-dimensional seismic dip section KK′, showing seismic recognition criteria for major paleogeographic types in the LM-T area. Section is located in Figure 1.

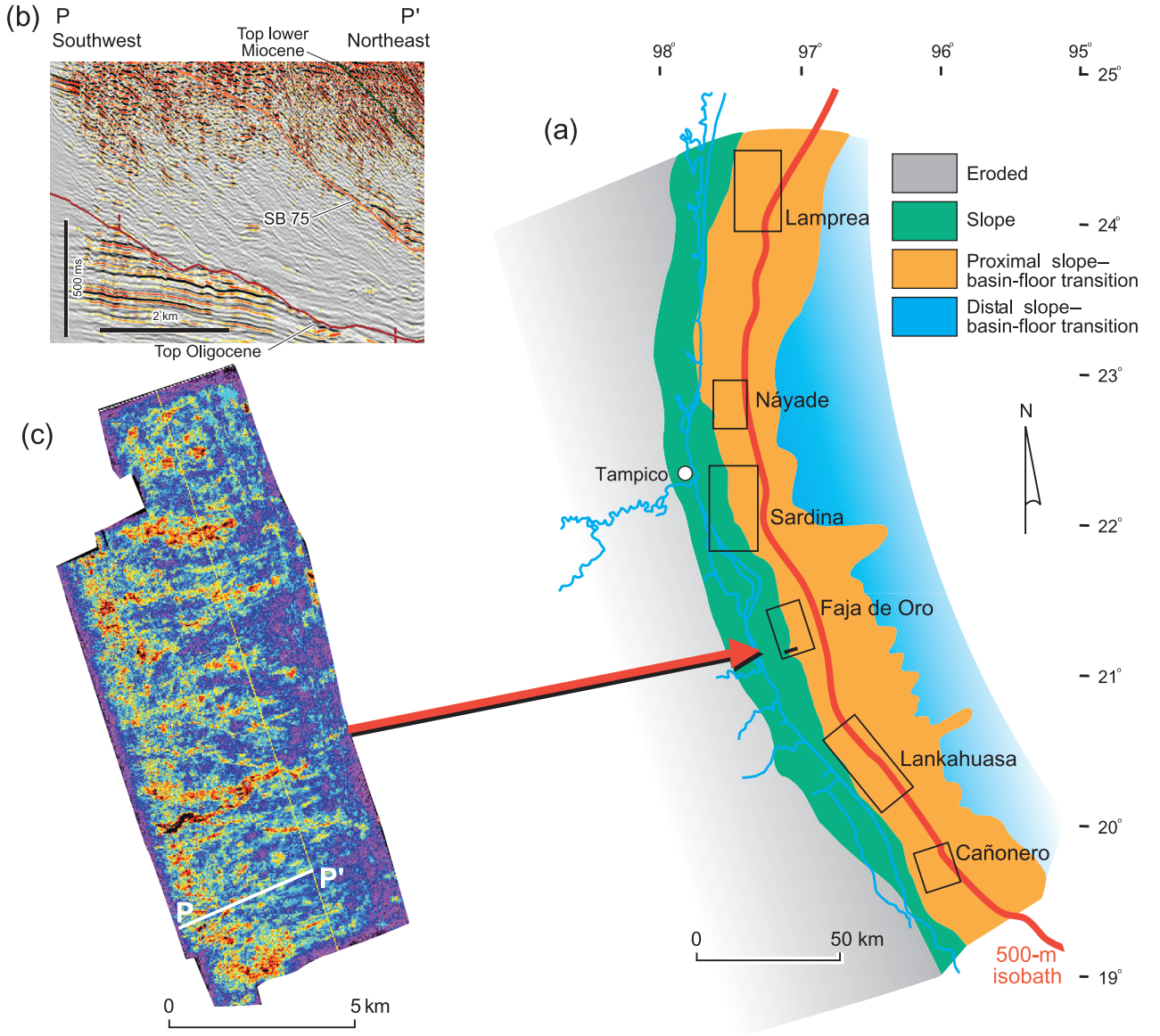

FIGURE 9. (a) Lower Miocene_1 paleogeography with slope and shelf deposits distributed updip (westward) of the 500-m (1600-ft) isobath. (b) Seismic dip section PP′ in the Faja de Oro 3-D survey, illustrating steeply dipping lower Miocene_1 slope deposits. Section is located in (c). The vertical exaggeration is approximately 3:1. (c) Maximum-amplitude map of the lower 80-ms interval in the lower Miocene_1 slope play in the Faja de Oro 3-D survey, illustrating narrow and dip-elongate slope-channel deposits.

However, south of the Lankahuasa 3-D survey, these shelf deposits are deeply dissected (locally >400 m [>1300 ft]) by a major lowstand canyon system in the area of Cañonero 3-D survey (Figure 10d).

Upper Pliocene slope deposits are located close to the modern 500-m (1600-ft) offshore isobath (Figure 11a). The upper Pliocene is interpreted to be eroded in an extensive area in the offshore from the Faja de Oro to the Sardina 3-D survey. The upper Pliocene section is complex in the Lamprea 3-D survey, where it consists of several shelf successions intercalated with inner slope slump deposits (Figure 11b).

PLAYS

Thirty-two plays mapped in the LM-T study are defined by eight age divisions and four types of paleogeographic settings. The eight age divisions, based on Petroleos Mexicanos biostratigraphic data and shown in Figure 3c, are (1) lower Miocene_1, (2) lower Miocene_2, (3) middle Miocene, (4) upper Miocene_1, (5) upper Miocene_2, (6) lower Pliocene, (7) middle Pliocene, and (8) upper Pliocene. The four main paleogeographic types (shelf, slope, canyon, and slope-to-basin-floor transition) in the LM-T area are discussed separately.

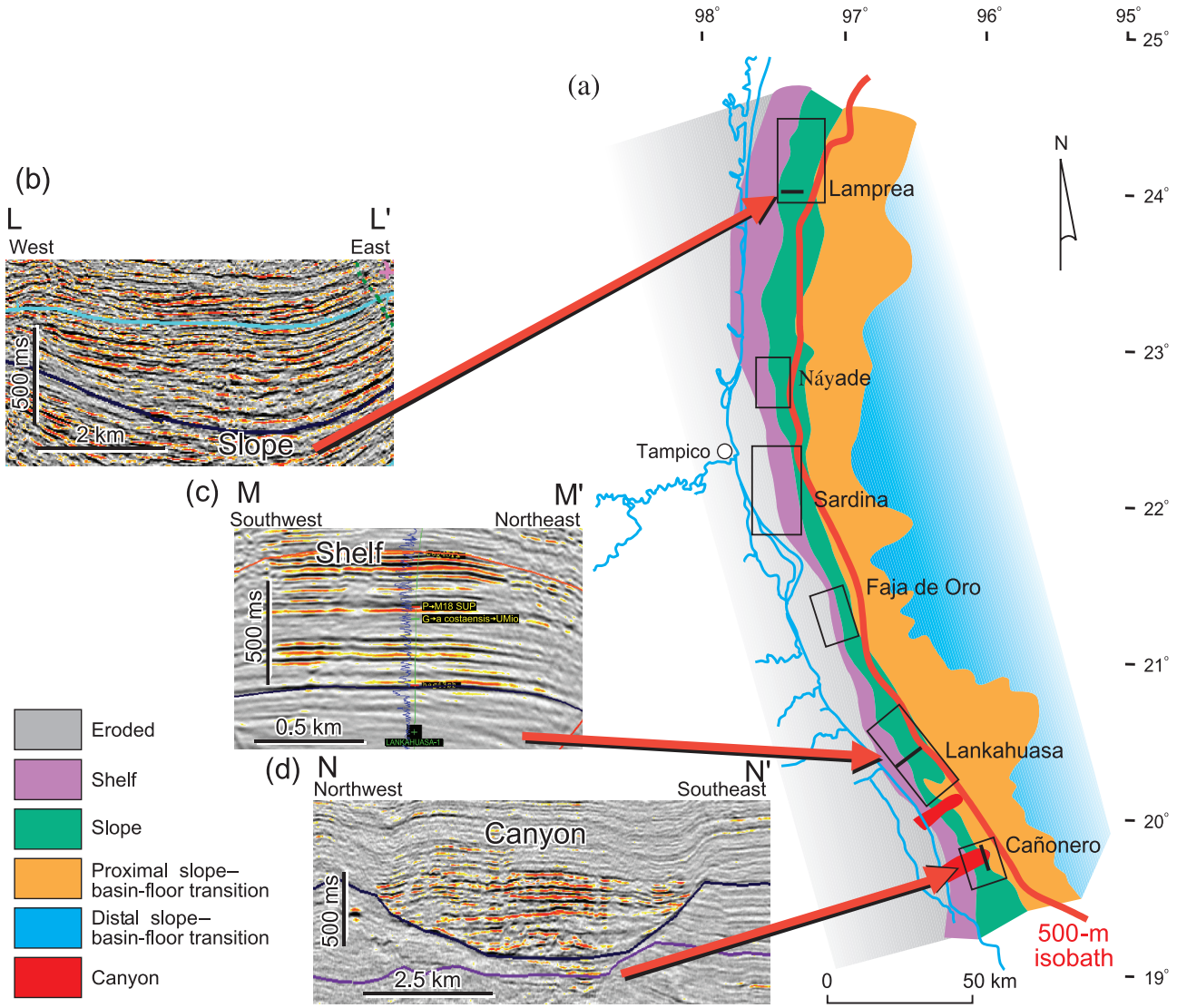

FIGURE 10. (a) Upper Miocene_2 paleogeography. (b) Three-dimensional seismic section LL′, showing mud-dominated, high-impedance slope deposits in the Lamprea 3-D survey. (c) Three-dimensional seismic section MM′, illustrating shelf successions in the Lankahuasa 3-D survey. (d) Three-dimensional seismic section NN′, portraying canyon-fill deposits in the Cañonero 3-D survey.

Shelf

Shelf plays defined in this study encompass a wide range of depositional environments, including coastal plain, shore zone, and submerged continental platform to the shelf edge. Shelf plays, as exemplified by the upper Miocene_2 shelf play in the Lankahuasa 3-D survey and trend, are typified by successions of thin sandstones with predominantly serrate log patterns (Figure 7a). Gas-bearing sandstones in the upper Miocene_2 shelf play in the Lankahuasa trend are common in transgressive systems tracts. These transgressive deposits are composed of strike-oriented isochron and amplitude patterns, indicating destruction and wave reworking of older deltaic and shoreface deposits (Figure 12a, b). Reservoir quality in these deposits is variable, where thin, burrowed sandstones (Figure 12c) pinch out into marine siltstone and mudstone. These sandstones are typically poorly sorted because of high amounts of muddy matrix introduced by burrowing. Common ichnofauna in these cores are Teichichnus, Rhizocorallium, Terebellina, and minor Thalassinoides. In contrast, Ophiomorpha and Skolithos are absent. Teichichnus, Rhizocorallium, Terebellina, and Thalassinoides can occur in a wide variety of water depths, but the absence of Ophiomorpha and Skolithos, common in sublittoral environments (Seilacher, 1967), indicates that the cored intervals are most likely from shelf, distal-deltaic, or lower shoreface settings.

A possible interpretation of upper Miocene_2 sandstones in the Lankahuasa trend includes shelf bars

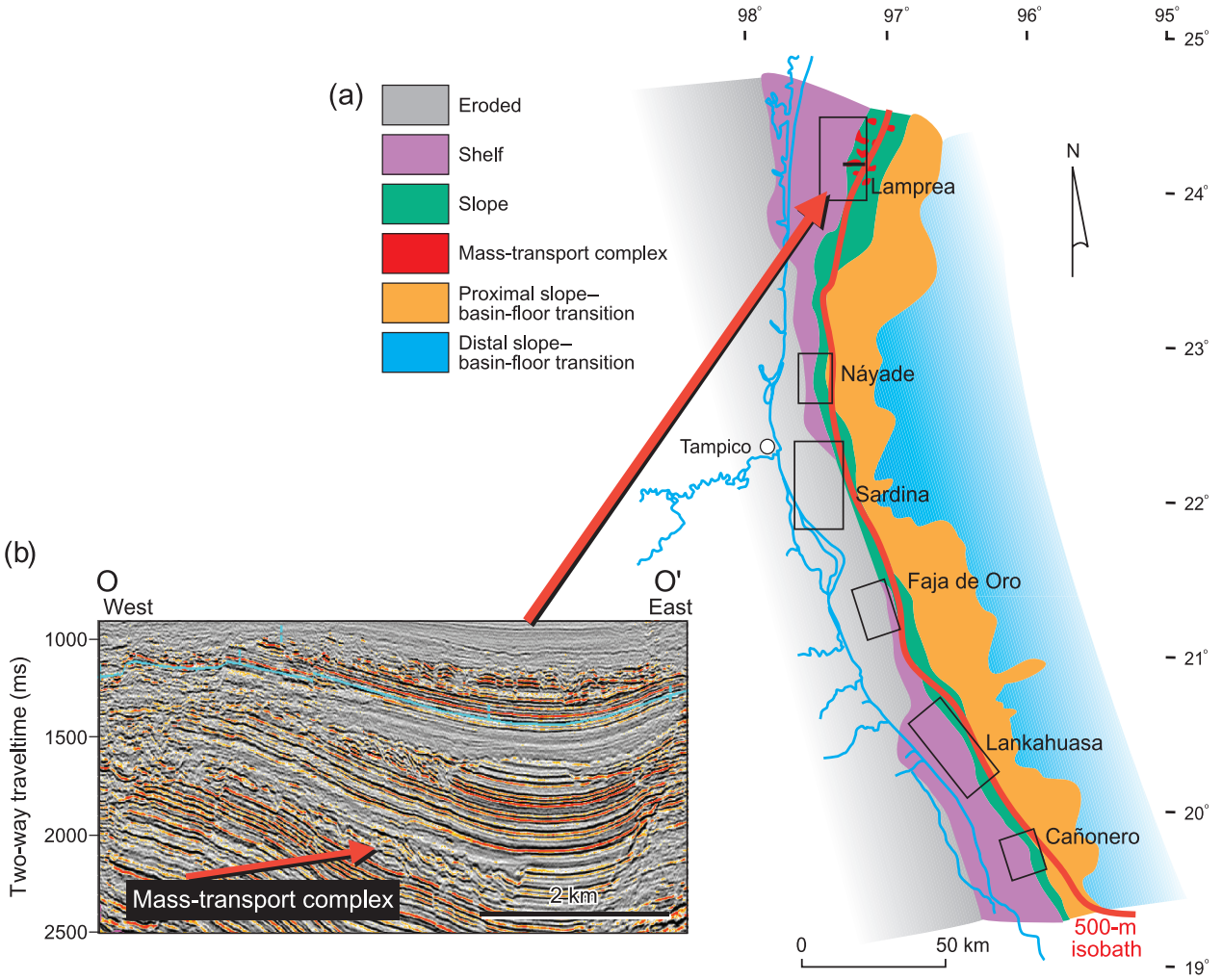

FIGURE 11. (a) Upper Pliocene paleogeography. (b) Three-dimensional seismic section OO′, showing inner slope slump deposits in the Lamprea 3-D survey.

because they are intensely burrowed and encased in marine mudstone and siltstone. However, these shelf sandstones may be reworked deposits from earlier lowstand progradational episodes (Figure 12d). During the SB43 lowstand, sandy deltaic sediments were inferred to have been delivered to an exposed outer shelf. These lowstand deltaic deposits were then reworked, burrowed by open-marine fauna, and subsequently stranded on the shelf during transgression in a sequence of events similar to those described by Plint (1988).

The upper Miocene outer shelf in the Lankahuasa trend is inferred from core and log data to have been a muddy, sediment-starved system of the type described by Kulm et al. (1975), despite the fact that the shelf was narrow. Logs of the Pliocene section in the Lankahuasa 3-D survey are dominated by successions of thin sandstones with serrate log responses, and percent-sandstone values computed from these logs are commonly less than 20%; thick, aggradational sandstones with blocky and blocky-to-upward-coarsening log signatures are absent. The muddy nature of the upper Miocene shelf in the Lankahuasa trend may have been the result of proximity to the trans-Mexican volcanic belt as well as the lack of large-scale depocenters. Additional investigations will be necessary to understand the influence of these factors on the upper Miocene shelf in this part of the LM-T area.

Slope

Slope plays in the LM-T area are typically mud dominated. Reservoir geometries consist of narrow, slightly sinuous, and dip-elongate channel and levee complexes. Reservoir quality is a major limiting factor in the LM-T slope plays, especially in the Tuxpan platform and adjacent areas, where many lower Miocene slope-channel sandstones are calcareous and with low porosity (Fouad et al., 2003a). These plays have a potential for stratigraphic traps, although potential reservoir size is limited.

The lower Miocene_1 slope play in the Faja de Oro 3-D survey is typical of other slope plays in the LM-T

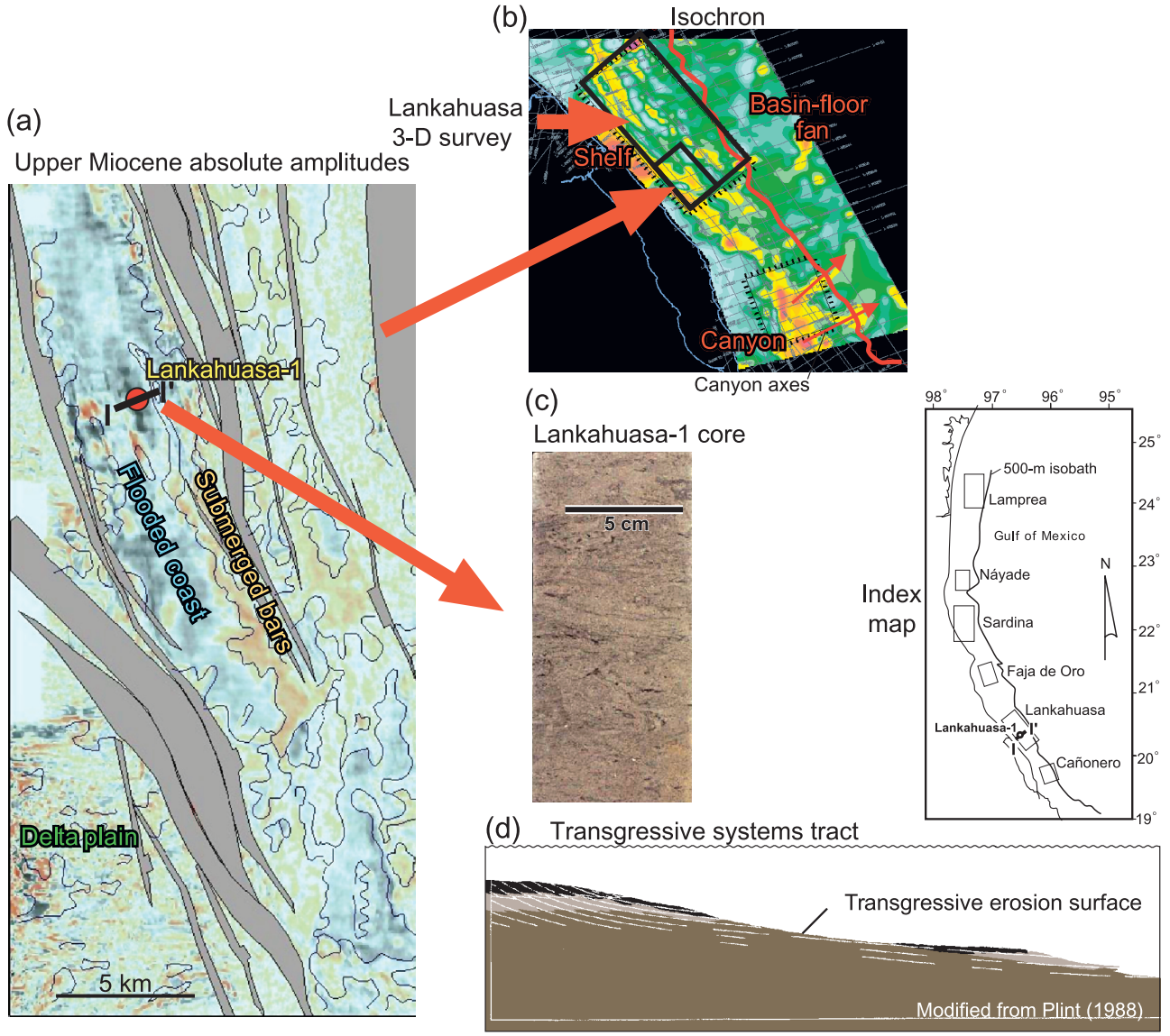

Figure 12. Upper Miocene_2 shelf systems in the Lankahuasa 3-D survey. (a) Absolute amplitude map of upper Miocene_2 transgressive deposits 40 ms below the FS40 maximum flooding surface, showing strike-parallel system of flooded coast and offshore submerged-bar deposits. (b) Isochron map of the upper Miocene_2 stratigraphic unit, with bright colors indicating thicker values. (c) Core from Pemex 1 Lankahuasa, showing heavily burrowed, fine-grained sandstones. (d) Model from Plint (1988), with in-place drowning and submergence of coastal deposits during transgression. Seismic section II′, indicated in (a), is shown in Figures 1 and 7a.

area. It consists of steeply dipping wedges and clinoforms above a major unconformity at the top of the Oligocene (Figure 9b). These strata commonly dip eastward at 10–15°, as measured on dip sections without vertical exaggeration. The internal architecture of the lower Miocene section is complex, consisting of numerous downlapping and crosscutting wedges.

A maximum-amplitude map of the interval 80 ms (~394 ft [~120 m]) above the top-of-Oligocene unconformity indicates that the bright-amplitude bodies are quite narrow (commonly only 0.3 mi [0.5 km] wide) and dip elongate, extending downdip (eastward) at least 3 mi (5 km) (Figure 9c). Eastward-merging tributary patterns are common, as well as pinch-outs downdip (basinward). A minor number of the bright-amplitude trends are sinuous, especially in the southern part of the Faja de Oro 3-D survey.

Canyon

Submarine canyon plays in the LM-T area are well developed in the upper Miocene_2 in the Cañonero trend (Figures 5, 6), where they are inferred to be related to periods of lowstand and associated with sediment bypass

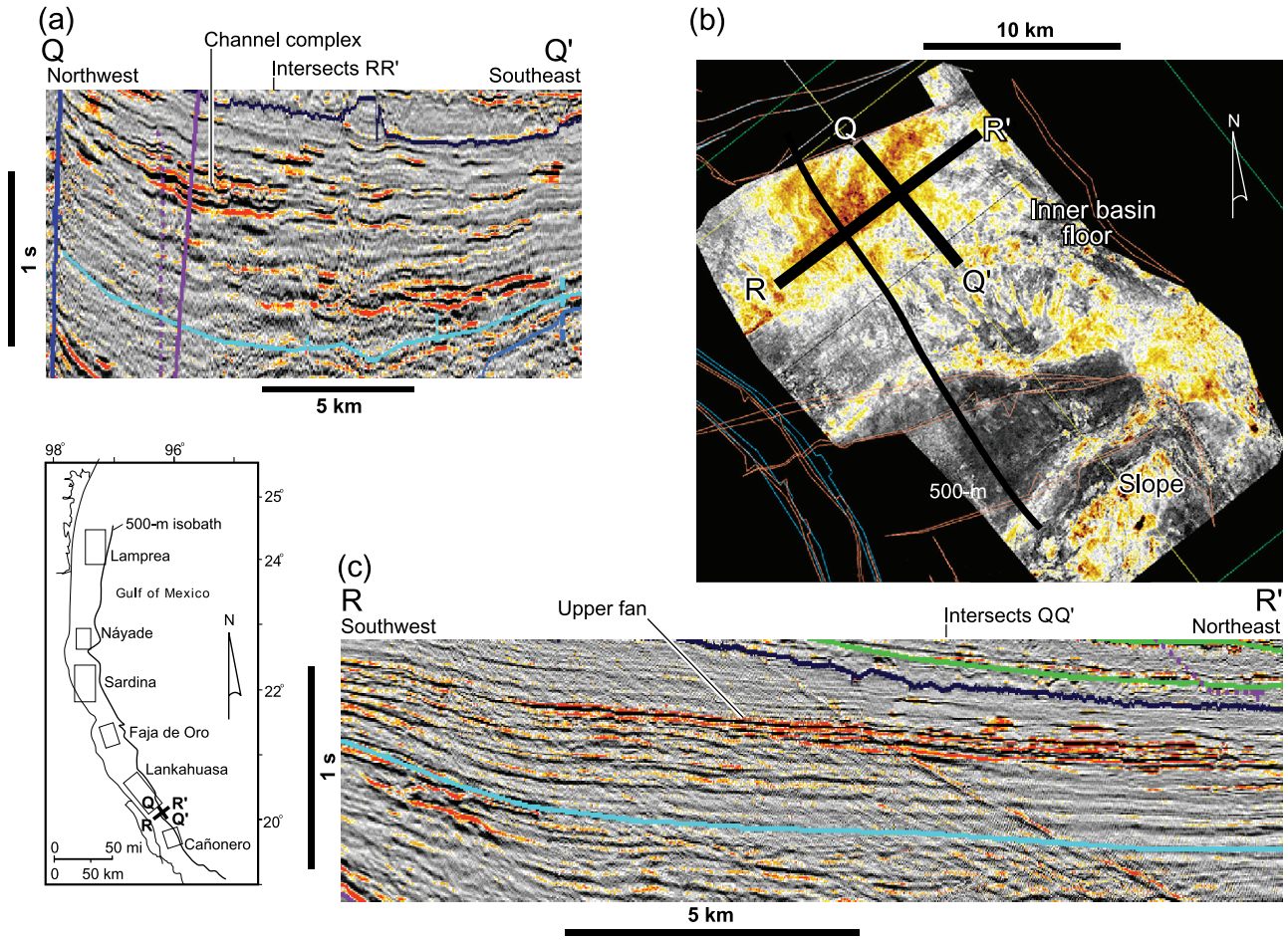

FIGURE 13. Upper Miocene_1 slope-to-basin-floor transition. (a) Three-dimensional seismic strike section QQ′, showing lenticular, bright-amplitude, and low-impedance slope-channel deposits. (b) Maximum peak amplitude map of slope-to-basin-floor transition above a local unconformity. (c) Three-dimensional seismic dip section RR′, displaying continuity of proximal-fan sheet deposits.

onto the basin floor (Ambrose et al., 2003a; Fouad et al., 2003b). They are defined as a single lenticular feature in strike section, varying in width from 5 to 8 km (3.1 to 5 mi), and are associated with 400–550 ms (480–660 m; 1574–2165 ft) of downcutting of older upper Miocene strata (Figure 5b, c). This canyon system has a wide variety of seismic responses and geometries that vary systematically from updip to downdip. For example, the updip trend is inferred to be mud prone, characterized by dim amplitudes, with locally chaotic reflectors along the margins possibly indicating slump facies (Figure 5a). In contrast, the downdip trend is composed of bright-amplitude strata that onlap onto the basal canyon unconformity (Figure 5b, c). The canyon system grades distally into basin-floor-fan deposits (Figure 6b), characterized by a dim- to moderate-amplitude set of parallel reflectors with minor onlap onto the unconformity (Figure 5d). Amplitudes in the Cañonero submarine canyon trend are incompletely understood because of only one well penetration at the time of this writing. Although the canyon fill has abundant bright-amplitude surfaces, these amplitudes may not indicate sandstone. Instead, they may indicate high-impedance tuffaceous deposits from the trans-Mexican volcanic belt.

Slope-to-Basin-Floor Transition

Slope-to-basin-floor transition plays in the LM-T area are developed mainly in the deeper offshore, east of the 500-m (1600-ft) isobath (Figures 6b, 13). These plays are inferred to contain thick (several hundred meters) channelized-lobe and extensive fan-sheet deposits. They commonly overlie regional unconformities and consist of bright-amplitude zones of wavy, subparallel reflectors capped by dim-amplitude flooding or fan-abandonment surfaces. These regional unconformities define individual episodes of lowstand-derived, submarine-canyon, and basin-floor-fan development that are interpreted to be tectonically driven, related to uplift in the Sierra Madre Oriental mountain belt. Reservoir quality in this play is expected to be highly variable, consisting of a variety of architectural elements, including fan lobes and sheets,

channel complexes and associated overbank deposits, and muddy interchannel areas (Figure 13).

Fan lobes and sheets are volumetrically the most significant component of the basin-floor plays, judging by analogy from similar plays in the adjacent Veracruz basin (Jennette et al., 2003). Trap sizes in these plays are large, especially in downdip, four-way closures associated with compressional toe thrusts at the distal end of growth faults. This combination of fan lobes and sheets, as well as larger trap sizes, makes this play one of the most favorable in the LM-T area, although reservoir quality in the Cañonero trend is inferred to be poor because of proximity to the trans-Mexican volcanic belt.

Play Elements

Neogene plays in the LM-T area are characterized by a variety of play elements, including reservoir presence and quality, trap, seal, source, migration, and timing, which together provide constraints on a play's chance of success. Criteria were developed separately for evaluating data from each play element, and data for assessing play elements were used from a wide variety of sources. The relative importance and adequacy of play elements vary greatly for LM-T plays (Table 1). For example, considerable differences exist in inferred reservoir quality among the plays because of diverse source terrains and facies variability. Great variations are also present in trap styles and trap density, reflecting different tectonic settings in each structural trend, ranging from compressional in the Cañonero trend to purely extensional with gravity-slide tectonics in the Lankahuasa and Faja de Oro trends, as well as halokinesis in the Lamprea trend. The migration potential, a function of the presence and distribution of deep-seated faults cutting into the primary Mesozoic source rocks, also varies greatly throughout the eastern Mexico Gulf Coast.

Reservoir Presence and Quality

Reservoir presence in the LM-T area was inferred from log response and observations of impedance character of reflectors from 3-D seismic data. Where these data were lacking or ambiguous, analogous data were used from the neighboring Veracruz basin. At the time of this writing, reservoir presence was documented for only two Neogene plays in the LM-T area: the upper Miocene_2 shelf in the Lankahuasa trend and the middle Miocene slope play in the Faja de Oro–Náyade trend. However, recent drilling activity in the Lankahuasa 3-D survey also indicates the presence of hydrocarbons in middle and lower Pliocene slope and shelf plays (Cuevas et al., 2004).

Reservoir quality in the LM-T plays was assessed directly from core data and indirectly from petrophysical calculations of average V_{sh} and average porosity from wells. Where these data were absent, additional inferences of reservoir quality were based on facies analogs from the Veracruz and Macuspana basins (Jennette et al., 2002, 2003; Ambrose et al., 2003b). Log computations were made over the entire play interval instead of individual sandstone beds to best represent the entire play interval. However, many of the well-based results of reservoir quality were deemed not to be representative of the plays because too few wells were present to adequately test the plays (Table 1). This is especially the case for middle and lower Miocene plays, in which the only available data were from the Sardina and Náyade 3-D survey areas.

Slope-to-basin-floor transition plays in the Cañonero trend and the Veracruz basin are inferred to contain thick, sandy, and conglomeratic successions in fan sheets and lobes, although reservoir quality may be limited by the presence of volcanic clays and muddy debris-flow deposits. Slope plays are inferred to be relatively muddier than the basin-floor plays, judging by abundant sidewall core data.

Trap

Traps in the LM-T plays were evaluated from size range and geographic distribution of closures mapped from seismic data. Plays with a small numbers of traps or limited trap density were deemed to have an unfavorable trap potential (Table 1). Many plays are currently inadequately tested for trap because of limited numbers of wells. Most closures west of the 500-m (1600-ft) isobath are three-way and fault bounded, ranging in size from less than 5 to more than 50 km^2 (1.9 to more than 19 mi^2). For example, the upper Miocene_2 gas-bearing zones in the western part of the Lankahuasa 3-D survey occur in a large ($\sim$60-km^2; $\sim$23-mi^2) closure, bounded updip (westward) by a major listric fault. Many of the four-way closures in the LM-T area occur along or downdip (east) of the 500-m (1600-ft) isobath associated with the Mexican Ridges fold belt.

Trap styles differ between each major LM-T structural trend. For example, many closures in the Cañonero trend are composed of three-way and small four-way traps associated with antithetic faults and inverted structures, respectively (Figure 4a). The most common closures in the Lankahuasa trend are three-way, fault-bounded traps, particularly in complexly faulted grabens (Figure 4b). Narrow, three-way, fault-bounded closures are common in the Faja de Oro–Náyade trend (Figure 4c). Closures in the Lamprea trend are a combination of three-way and four-way types, reflecting the presence of mobile shale and salt structures (Figure 4d).

Although delineation of stratigraphic traps was beyond the scope of this regional project, there is a potential for such traps in the LM-T area, especially in the deep-water slope, canyon, and slope-to-basin-floor transition plays. The sandstone architecture of the slope

plays, typified by the lower Miocene_1 slope play in the Faja de Oro and Sardina 3-D surveys, is complex, consisting of a dip-elongate network of narrow channel-fill and levee deposits pinching out into low-permeability mudstones and siltstone and which exhibit multiple pinch-outs (Fouad et al., 2003a) (Figure 13). Similarly, pinch-outs of canyon-fill deposits in the Cañonero trend are common, although the reservoir quality of these canyon-fill deposits may be limited by volcanic detritus from the updip trans-Mexican volcanic belt. The LM-T slope-to-basin-floor transition plays in the Cañonero trend are hypothesized to have a good potential for stratigraphic traps, particularly in the proximal facies tract, with stratigraphic compartmentalization related to complex channelized-fan deposits (Jennette et al., 2003).

Seal

Data from wells are insufficient to test many LM-T plays (Table 1). However, overpressure data from a few wells indicate that most overpressured zones occur in the middle and lower Miocene. Moreover, there may be differences in potential top seal among LM-T plays, inferred from variations in thickness of shales above flooding surfaces and fan-abandonment surfaces. For example, the middle Miocene is overlain by a thick succession of slope shales that should provide an excellent opportunity for vertical seal (Figure 7b). In contrast, the Pliocene section, especially in the Lankahuasa trend, is composed of sandy shelf and inner slope systems, with thin, intervening intervals of shale that may provide poor top seal (Figure 4b).

Seal in LM-T plays could potentially be compromised in areas intersected by major deep-seated faults. Many of these deep-seated faults are associated with current seafloor gas and oil seeps. In addition, intensely faulted zones that may contain numerous fractures, for example, the heavily faulted grabens in the east-central Lankahuasa 3-D survey (Figure 4b), may have a seal risk.

Source

Source, inferred from distribution, thickness, and thermal maturity of Tithonian deep-water shales in 46 wells in onshore and nearshore areas of the eastern Mexico Gulf Coast, is deemed adequate for all LM-T Neogene plays. Calcareous shales and argillaceous limestones of the three Upper Jurassic units (Oxfordian, Kimmeridgian, and Tithonian) contain abundant good to excellent type II oil-prone source rocks with TOC of 2% and higher and hydrogen index (HI) between 400 and 600 mg HC/g TOC. The Upper Jurassic source rocks are mature to overmature in the offshore LM-T area and are inferred to have generated and expelled large quantities of oil and gas. The Tithonian is one of the most important source rock units of the Upper Jurassic, based on its source characteristics, net thickness, and regional distribution, as well as for its widespread contribution to oil accumulations (Jordan and Wilson, 2003). Upper Jurassic samples from the onshore areas are immature to mature. We have estimated an original (i.e., prior to maturation) TOC of 3% and an original HI of 600 mg HC/g TOC for the Tithonian type II source rocks, which are used in maturity and hydrocarbon generation models.

Greater thicknesses of the Upper Jurassic were mapped in 12 grabens in the Tampico-Misantla basin by Román-Ramos and Holguín-Quiñones (2001). They estimated an average TOC of 2.2%, HI of 500 mg HC/g TOC, and thickness of 550 m (1800 ft) for the Upper Jurassic. Tithonian and Oxfordian units are interpreted to contain the richest source rock intervals in the Upper Jurassic, and the Kimmeridgian is a less important source rock unit.

Román-Ramos and Holguín-Quiñones (2001) mapped TOC enrichments in the Poza Rica area, the Tuxpan platform, and Arenque area in the Sardina 3-D survey. Jordan and Wilson (2003) evaluated TOC and pyrolysis data of approximately 800 samples from 100 wells in the Burgos, Tampico-Misantla, and Sureste basins of Mexico. They found that source rock TOC averaged as much as 3–4% in these basins. Based on estimations of the vertical extent of this richness by log-derived TOC calculations, they suggested that most of the Tithonian section is of source rock richness, except for some transitional beds at the base of the section.

Forty oil shows with similar gas-composition characteristics were identified in this study from ocean-bottom sediment cores from the Lankahuasa and Lamprea 3-D surveys and from areas north of Lankahuasa 3-D survey. Four of these oil shows have been correlated in this study, based on biomarkers (terpanes and steranes) and carbon isotope data with Tithonian-sourced oils from the Tampico-Misantla basin described by Guzmán-Vega et al. (2001). This oil show–source correlation indicates the presence of oil-prone Tithonian source rocks in the subsurface and the existence of an active Upper Jurassic petroleum system in the LM-T offshore area. A maturity reconstruction of the Upper Jurassic in the offshore LM-T study area suggests that the Tithonian source rocks are presently mature to overmature (Figure 14). Assuming a source quality similar to that of the onshore areas (which is quite likely), it can be inferred that the Tithonian sources have generated and expelled large quantities of oil and gas in the offshore areas. Gases produced from upper Miocene sandstones in the Lankahuasa 3-D survey and several gas shows from north of Lankahuasa have been identified in this study as dry, very mature thermogenic gases (R_o about 2.0% and higher) based on molecular and carbon isotope compositions.

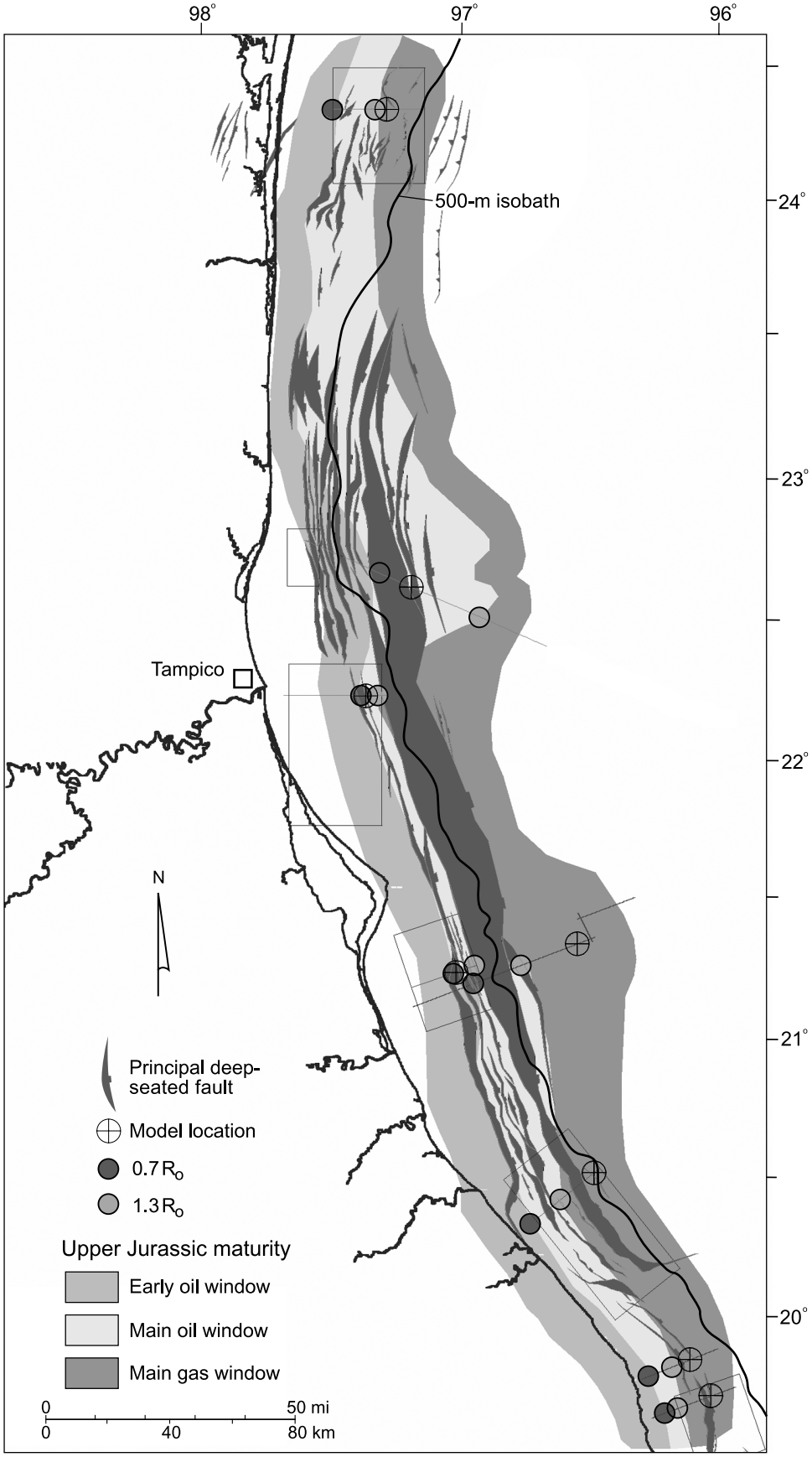

FIGURE 14. Upper Jurassic maturity in the LM-T area, based on calculations of vitrinite reflectance (R_o) in eight model locations.

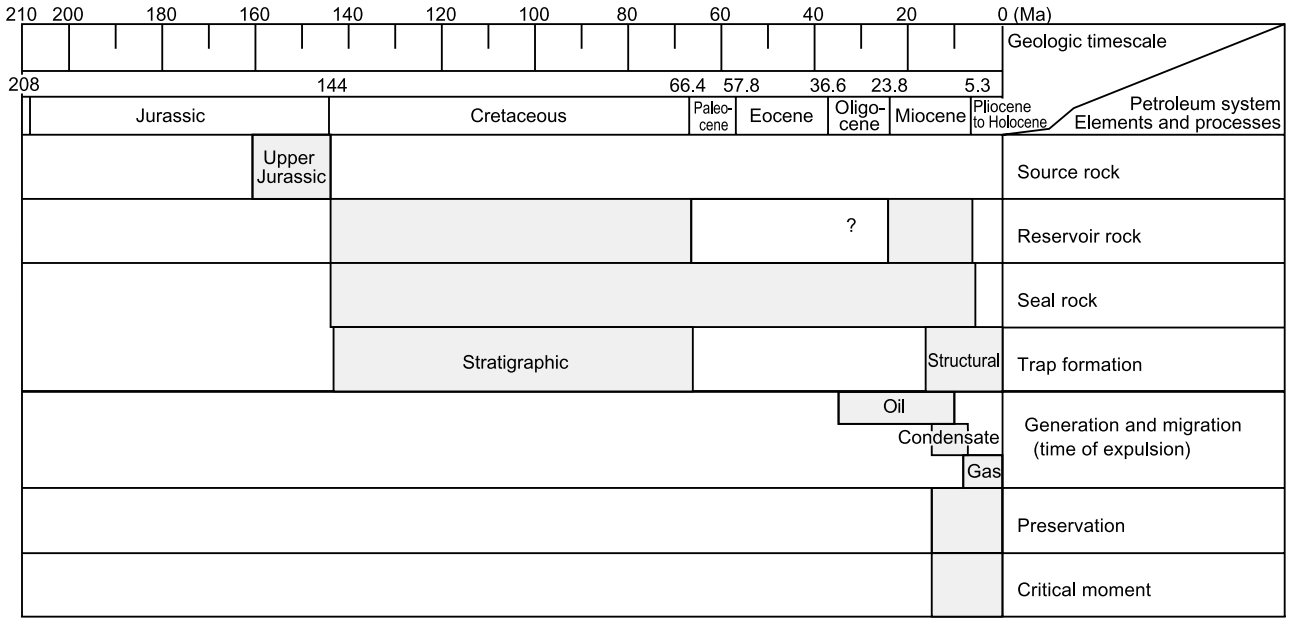

FIGURE 15. Upper Jurassic petroleum system chart for the Lankahuasa trend.

In contrast with the Tithonian section, Cretaceous and Tertiary strata have only a limited potential for providing hydrocarbon sources. The Cretaceous succession contains mostly carbonate reservoir rocks with minor intervals of calcareous shales and argillaceous limestones. Evaluation of these source rocks shows fair to good TOC contents (mostly between 0.50 and 1.5%, average 0.95%) and mostly type II oil-prone and type II/III oil- and gas-prone kerogens (HI 400–600 and 200–400 mg HC/g TOC, respectively). Potential Cretaceous source rocks are mostly immature in the onshore areas. Paleogene shales evaluated from the onshore areas show only immature, poor gas source rocks. Neogene (Miocene and Pliocene) shales are identified as minor biogenic gas source rocks.

Migration and Timing

Source rock evaluation suggests that the possibility of hydrocarbon charge from the deep Upper Jurassic source is a necessary condition for large gas accumulations in LM-T Neogene plays. Therefore, it is critical that vertical migration paths existed and large quantities of gas were available for migration when Neogene traps formed.

Variations in migration potential, inferred from the geometry of deep-seated faults likely to tap the predominant Upper Jurassic source, exist among the various LM-T trends. For example, the Cañonero trend contains numerous basement-involved faults inferred to provide direct upward-migration pathways from the Mesozoic to the Neogene. In contrast, areas north of the Cañonero trend and downdip of principal listric faults are problematic for upward migration of Mesozoic-sourced hydrocarbons. These listric faults have a nearly horizontal detachment surface above the top of the Mesozoic, soling out into Oligocene shales. Areas updip of the large-scale listric fault systems contain plays that are intersected by major faults cutting the ancestral Cretaceous shelf edge and that are directly connected to Mesozoic source rock intervals.

Timing was assessed from hydrocarbon modeling from several locations throughout the LM-T area, primarily in the shallow offshore. Input parameters for these models included stratigraphic and lithologic data, temperature and thermal-history data, and geochemical parameters, such as thermal-maturity data, bottomhole temperature and heat-flow data, HI and primary oil and gas potential, kerogen-to-oil and oil-to-gas kinetics, thermal-maturity data, hydrocarbon type, and isotopic data. Ages and lithologic compositions for the Paleogene, Cretaceous, and Upper Jurassic intervals were obtained from publications and from Petroleos Mexicanos data.

Timing is not a limiting play element for the LM-T plays because nearly all areas have experienced recent (5.0 Ma and younger) expulsion of hydrocarbons. However, some variations are present in the timing of hydrocarbon expulsion and trap formation between different trends in the LM-T area. These variations do not affect play possibilities but may have an impact on the probability of success of each prospect.

The Upper Jurassic petroleum system chart for the Lankahuasa trend is given as an example, where oil, condensate, and main gas generation and migration from the Upper Jurassic oil source (oil-prone type II) occurred

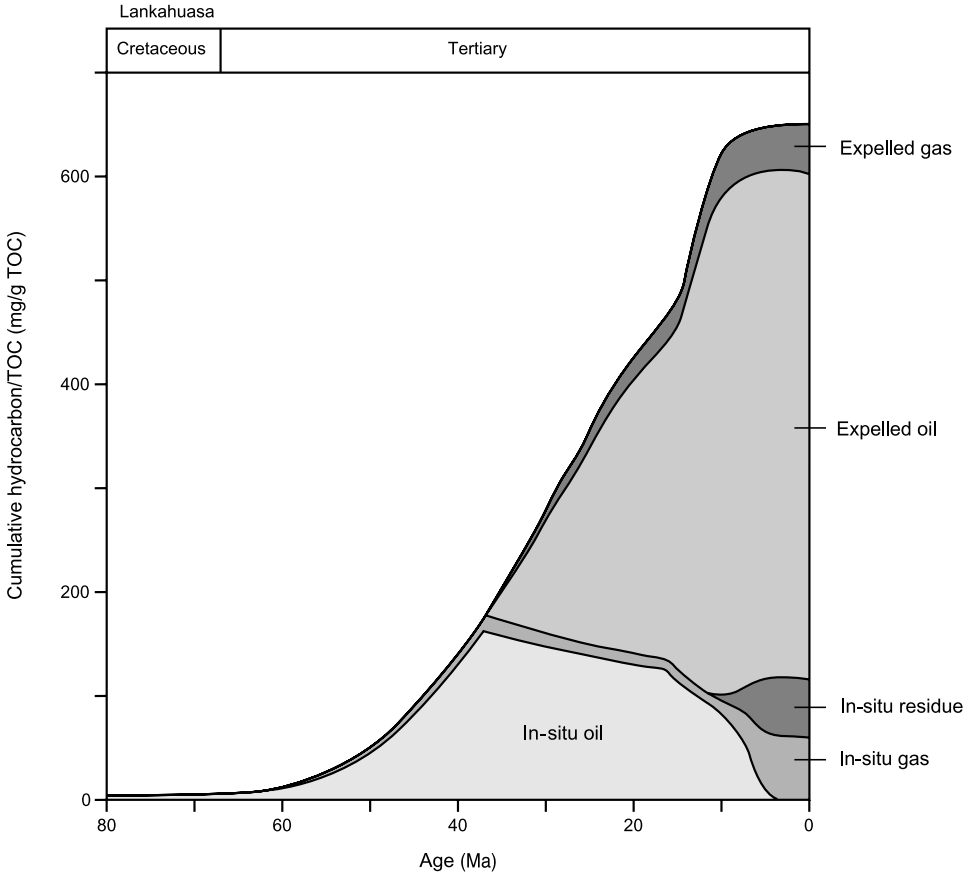

FIGURE 16. Cumulative oil and gas generation and expulsion vs. geologic time for the upper Jurassic source in the Lankahuasa trend.

during the Oligocene to middle Miocene (35.0–11.5 Ma), middle Miocene to late Miocene (13.0–7.8 Ma), and late Miocene to Holocene (9.6–0 Ma), respectively (Figure 15). Hydrocarbon types that could migrate from the source into Neogene plays during the development of traps and migration paths (16.4–0 Ma) are oil, condensate, and gas. During intense early Pliocene faulting, only gas could migrate from the source into Neogene plays. Listric faults in this trend detach above the source rock interval. As a result, vertical, cross-stratal, fault-related migration conduits connecting Jurassic source rocks with Neogene reservoirs and traps are interpreted to be a significant risk in this trend.

Most of the oil in the Lankahuasa trend is inferred to have been generated and expelled during the 35.0–16.4 Ma period prior to Neogene trap formation (Figure 16). Therefore, the quantity of hydrocarbons (oil, condensate, and gas) that could migrate directly from the source during Neogene trap formation was relatively much less important compared to the quantity of oil expelled from the source prior to Neogene trap formation (Figure 16), when the source was at about 0.70–0.85% R_o maturity and was in the main oil window (Figure 17).

In the other LM-T trends, starting in the south with the Cañonero trend, oil, condensate, and main gas generation and expulsion from the Upper Jurassic source occurred during middle Eocene to late Oligocene (47.0–27.0 Ma), early Oligocene to early Miocene (31.5–18.0 Ma), and early Miocene to Holocene (22.0–0 Ma), respectively. Hydrocarbon types that could migrate into Neogene plays during trap formation in the late Miocene to Holocene (10.2–0 Ma) were gas from the Upper Jurassic source rock intervals.

In the Faja de Oro–Náyade trend, oil generation and expulsion from the Upper Jurassic source occurred during middle Miocene to Holocene (10.2–0 Ma). In the Faja de Oro 3-D survey, formation of Neogene traps occurred during the middle Miocene to middle Pliocene (16.4–3.4 Ma). Therefore, oil could have migrated into Neogene traps. In the Sardina 3-D survey area, oil generation and expulsion from the Upper Jurassic source occurred during the late Miocene to Holocene (6.5–0 Ma). Traps in the Neogene intervals formed during the middle Miocene (16.4–10.2 Ma). In the Náyade 3-D survey area, oil generation and expulsion from the Upper Jurassic source occurred during the late Miocene to Holocene (11.0–0 Ma). Neogene traps formed during the middle Miocene–Holocene (16.4–0 Ma).

In the Lamprea trend, oil, condensate, and main gas generation and expulsion from the Upper Jurassic source occurred during the early Miocene to middle late Miocene (18.0–5.3 Ma), the late Miocene to late Pliocene (7.2–2.0 Ma), and the middle Pliocene to Holocene

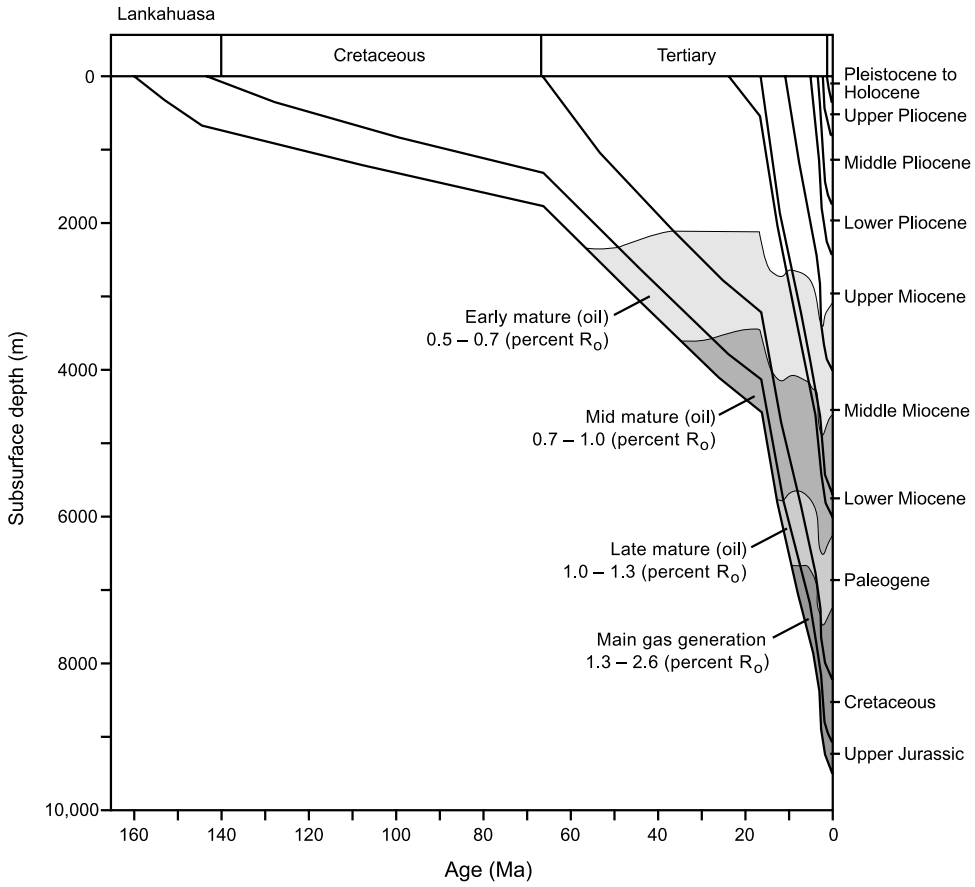

FIGURE 17. Burial-history diagram with thermal-maturity windows for the Lankahuasa trend.

(3.3–0 Ma), respectively. If fault-related migration paths were available, the hydrocarbon types that could migrate from the Upper Jurassic source intervals into Neogene plays during trap formation in the late Miocene to late Pliocene (6.0–1.8 Ma) would consist of light oil, condensate, and gas.

SUMMARY

Neogene shelf, slope, canyon, and slope-to-basin-floor transition plays in the LM-T continental shelf are controlled by a variety of structural and stratigraphic features, including gravity sliding and extension, compression and strike-slip motion, salt evacuation, and formation of lowstand canyon and fan systems associated with major uplift and incision of the Sierra Madre Oriental mountain belt. The Lankahuasa trend, discussed first in this summary, has the greatest overall potential of all the LM-T trends, considering it contains a greater number of already proven plays, as well as an array of more favorable play elements (Table 1). The other trends (Cañonero, Faja de Oro–Náyade, and Lamprea) have a similar overall but lesser potential than the Lankahuasa trend and are discussed in geographical order from south to north.

At the time of this writing, the Lankahuasa trend has two proven plays, the upper Miocene_2 shelf and the lower Pliocene slope. Reservoir quality in the upper Miocene_2 shelf play is adequate, although individual sandstones in the play are thin and contain a wide range of porosity values (10–25%). However, these data are currently unavailable for the lower Pliocene slope play. Trap types for both plays are similar, being three-way and fault bounded above a system of major shallow-detachment listric faults. Seal is provided by laterally continuous flooding surfaces and slope mudstones, in combination with fault offsets, locally in excess of 100 m (330 ft). However, seal may be compromised locally in intensely faulted and fractured grabens in the eastern part of the Lankahuasa 3-D survey (Figure 4b). Migration in the Lankahuasa trend is adequate because of the existence of proven plays and the widespread presence of oil and gas seeps in the area.

Plays in the Cañonero trend contain a wide variety of favorable, unfavorable, and untested play elements (Table 1). Reservoir presence and quality have yet to be demonstrated for all plays in the Cañonero trend, and recent drilling activity in the upper Miocene_2 canyon play suggests the presence of volcanogenic deposits. Although trap is currently untested in the shelf and slope plays, abundant three-way and areally limited four-way

closures are hypothesized to exist in the shelf-to-basin-floor transition and canyon plays. Seal is expected to be favorable in the slope-to-basin-floor transition and canyon plays, where thick, dim-amplitude successions of shale are inferred to overlie flooding and fan-abandonment surfaces (Figures 5, 7b). Source, migration, and timing are deemed to be favorable play elements in the Cañonero trend, where deep-seated basement faults are inferred to have provided upward migration for hydrocarbons.

The Faja de Oro–Náyade trend contains only one Neogene play where reservoir presence has been demonstrated, occurring in thin, silty sandstones in the middle Miocene slope play (Table 1). The western part of the Faja de Oro–Náyade trend is dominated by thick successions of steeply dipping lower and middle Miocene slope plays containing narrow channel and levee complexes (Figure 9). Traps in these slope plays are defined by narrow, three-way closures against faults (Fouad et al., 2003a). The source in the western part of the Faja de Oro–Náyade trend is expected to be predominantly oil, and migration pathways are inferred to be provided by major fault systems developed along the ancestral Cretaceous carbonate shelf margin, west of the Faja de Oro fault (Figure 4c). Major listric faults in the downdip Faja de Oro–Náyade trend are interpreted to sole out into Oligocene shales, above the primary Mesozoic source, and therefore, migration in this part of the trend is problematic and untested.

The Lamprea trend, like the Faja de Oro–Náyade trend, contains a great number of untested play elements (Table 1). Reservoir quality is deemed to be adequate in the shallow, uncompacted shelf plays, but a recently drilled well in more deeply buried plays, such as the middle Miocene slope play, indicates low porosity values because of high siltstone content, calcite cement, and compaction. A great variety of trap types exists in the Lamprea trend, consisting of three-way, fault-dependent traps in the updip Miocene extensional complex (Figure 4d), sparse four-way traps in the downdip, eastern part of the trend, and areally limited traps associated with diapirs. Seal is untested for almost all of the plays, except for the middle Miocene slope play (Table 1). Source is inferred to be favorable, but potential migration pathways may be compromised by impermeable salt and mud diapirs, as well as salt welds.

ACKNOWLEDGMENTS

The Bureau of Economic Geology, John A. and Katherine G. Jackson School of Geosciences, University of Texas at Austin, acknowledges support of this research by Landmark Graphics Corporation via the Landmark University Grant Program. Partial support for this publication was received from the John A. and Katherine G. Jackson School of Geosciences and the Geology of Foundation of the University of Texas at Austin.

This report was funded by Petroleos Mexicanos Exploración y Producción under Contract No. PEP-RN-RDIE-072/02-P. The Bureau of Economic Geology appreciates the opportunity to contribute to Petroleos Mexicanos' assessment of the hydrocarbon resources of the southern Laguna Madre–Tuxpan continental shelf and the continuous help and project participation by management and geoscientists of the Coordinación de Exploración at Poza Rica and the Asset Office at Tampico. Significant coordination between Petroleos Mexicanos and the Bureau of Economic Geology was facilitated by Luis Sanchez-Barreda.

The manuscript benefited greatly from the reviews of Robert M. Mitchum, William E. Galloway, Paul Post, and Eric Potter. Manuscript editing was by Lana Dieterich. Pat Alfano prepared the illustrations under the direction of Joel Lardon, manager, Media Information Technology. Publication was authorized by the director of the Bureau of Economic Geology.

REFERENCES CITED

Ambrose, W. A., et al., 2003a, Miocene valley-fill, slope, and submarine-canyon systems in the Laguna Madre–Tuxpan area, Mexico: Gulf Coast Association of Geological Societies Transactions, v. 53, p. 11–18.

Ambrose, W. A., et al., 2003b, Geologic framework of upper Miocene and Pliocene gas plays of the Macuspana basin, southeastern Mexico: AAPG Bulletin, v. 87, no. 9, p. 1411–1435.

Beaubouef, R. T., C. R. Rossen, F. B. Zelt, M. D. Sullivan, D. C. Mohrig, D. C. Jennette, J. A. Bellian, S. J. Friedman, R. W. Lovell, and D. S. Shannon, 1999, Deep-water sandstones, Brushy Canyon Formation, west Texas: AAPG Continuing Education Course Notes Series 40, variously paginated.

Buffler, R. T., 1983, Structure of the Mexican Ridges fold belt, southwest Gulf of Mexico, *in* A. W. Bally, ed., Seismic expression of structural styles; a picture and work atlas; v. 2: AAPG Studies in Geology 15, p. 2.3.3-16–2.3.3-21.

Buffler, R. T., and D. S. Sawyer, 1985, Distribution of crust and early history, Gulf of Mexico basin: Gulf Coast Association of Geological Societies Transactions, v. 35, p. 333–344.

Cuevas, J. A., M. Aranda Garcia, J. R. Román-Ramos, and J. Morales-Marin, 2004, Historical synopsis and geological framework of hydrocarbon plays, continental shelf, southwestern Gulf of Mexico (abs.): AAPG Annual Meeting Program, v. 13, p. A30.

Feng, J., R. T. Buffler, and M. A. Kominz, 1994, Laramide orogenic influence on late Mesozoic–Cenozoic subsidence history, western deep Gulf of Mexico basin: Geology, v. 22, p. 359–362.

Ferrari, L., M. López-Martínez, G. Aguirre-Diaz, and G. Carrasco-Nuñez, 1999, Space-time patterns of Cenozoic arc volcanism in central Mexico: From the Sierra Madre Occidental to the Mexican volcanic belt: Geology, v. 27, no. 4, p. 303–306.

Fouad, K., W. A. Ambrose, S. Sakurai, and D. Jennette, 2003a, Wave-shape classification and attribute analysis of the lower Miocene deep-water reservoirs, Madre basin, offshore Mexico (ext. abs.): Society of Exploration Geophysics Transactions, Seventy-Third Annual Meeting and International Exposition, CD-ROM, 4 p.

Fouad, K., W. A. Ambrose, F. Brown, and D. Jennette, 2003b, Seismic facies an attribute analysis of the Miocene incised-valley and submarine-canyon systems in Tuxpan basin, offshore Mexico (ext. abs.): Society of Exploration Geophysicists Seventy-Third Annual Meeting and International Exposition, CD-ROM, 4 p.

Galloway, W. E., P. E. Ganey-Curry, X. Li, and R. T. Buffler, 2000, Cenozoic depositional history of the Gulf of Mexico basin: AAPG Bulletin, v. 84, p. 1743–1774.

Goldhammer, R. K., and C. A. Johnson, 2001, Middle Jurassic–Upper Cretaceous paleogeographic evolution and sequence-stratigraphic framework of the northwest Gulf of Mexico rim, *in* C. Bartolini, R. T. Buffler, and A. Cantu-Chapa, eds., The western Gulf of Mexico basin: Tectonics, sedimentary basins, and petroleum systems: AAPG Memoir 75, p. 45–81.

González, R., and N. Holguín, 2001, Las rocas generadoras de Mexico: Asociación Mexicana de Geólogos Petroleros, v. 49, no. 1–2, p. 16–30.

Guzmán-Vega, M. A., and M. R. Mello, 1999, Origin of oil in the Sureste basin, Mexico: AAPG Bulletin, v. 83, no. 7, p. 1068–1095.

Guzmán-Vega, M. A., L. Castro Ortiz, J. R. Román-Ramos, L. Medrano-Morales, L. C. Valdez, E. Váquez-Covarrubias, and G. Ziga-Rodríguez, 2001, Classification and origin of petroleum in the Mexican Gulf Coast basin: An overview, *in* C. Bartolini, R. T. Buffler, and A. Cantu Chapa, eds., The western Gulf of Mexico basin: Tectonics, sedimentary basins, and petroleum systems: AAPG Memoir 75, p. 127–142.

Haq, B. U., J. Hardenbol, and P. R. Vail, 1987, Chronology of fluctuating sea levels since the Triassic: Science, v. 235, p. 1156–1166.

Jennette, D., T. Wawrzyniec, K. Fouad, D. Dunlap, J. Meneses-Rocha, F. Grimaldo, R. Muñoz, D. Barrera, C. Williams-Rojas, and A. Escamilla-Herrera, 2003, Traps and turbidite reservoir characteristics from a complex and evolving tectonic setting, Veracruz basin, southeastern Mexico: AAPG Bulletin, v. 87, no. 10, p. 1599–1622.

Jennette, D. C., et al., 2002, Play-element characterization of the Miocene and Pliocene Veracruz basin, southeastern Mexico: Gulf Coast Association of Geological Societies Transactions, v. 52, p. 441–454.

Jordan, C. L., and J. L. Wilson, 2003, Geologic controls on the organic richness of Tithonian (Upper Jurassic) source rocks in the Burgos, Tampico-Misantla, and Sureste basins of Mexico, *in* N. E. Rosen, ed., Structure and stratigraphy of south Texas and northeast Mexico: Applications to exploration: Gulf Coast Section SEPM Foundation and South Texas Geological Society, Special Publication, CD-ROM, p. 22–24.

Kulm, L. D., R. C. Rousch, J. C. Harlett, R. H. Neudeck, D. M. Chambers, and E. J. Runge, 1975, Oregon continental shelf sedimentation: Interrelationships of facies distribution and sedimentary processes: Journal of Geology, v. 83, p. 145–176.

Magoon, L. B., T. L. Hudson, and H. E. Cook, 2001, Pimienta-Tamabra, a giant supercharged petroleum system in the southern Gulf of Mexico, onshore and offshore Mexico, *in* C. Bartolini, R. T. Buffler, and A. Cantú-Chapa, eds., The western Gulf of Mexico basin: Tectonics, sedimentary basins, and petroleum systems: AAPG Memoir 75, p. 83–125.

Marton, G., and R. T. Buffler, 1994, Jurassic reconstruction of the Gulf of Mexico basin: International Geology Review, v. 36, p. 545–586.

Mello, M. R., et al., 1996, Geochemical characterization of oils from the Gulf of Mexico and southeastern Mexican basins: A petroleum system approach to predict deep water probes, *in* E. Gómez-Luna and A. M. Cortez, eds., 5th Latin American Congress of Organic Geochemistry, Cancún, Mexico, Memoir, Abstracts Volume, p. 106–109.

Pew, E., 1982, Seismic structural analysis of deformation in the southern Mexican ridges: M.A. Thesis, University of Texas at Austin, Austin, 101 p.

Pindell, J. L., 1994, Evolution of the Gulf of Mexico and the Caribbean, *in* S. K. Donovan and T. A. Jackson, eds., Caribbean geology: An introduction: Kingston, Jamaica, UWI Publishers, p. 12–39.

Pindell, J. L., L. Kennan, and S. Barrett, 2000, Putting it all together again: AAPG Explorer, v. 21, p. 58–62.

Plint, A. G., 1988, Sharp-based shoreface sequences and ''offshore bars'' in the Cardium Formation of Alberta: Their relationship to relative changes in sea level, *in* C. K. Wilgus, B. S. Hastings, H. Posamentier, J. Van Wagoner, C. A. Ross, and C. G. St. C. Kendall, eds., Sea level changes, an integrated approach: SEPM Special Publication 42, p. 357–370.

Román-Ramos, J., R. E. Mena-Sánchez, and L. Bernal-Vargas, 1996, Evaluación geoquímica de los recursos petrolíferos de la Cuenca Tampico-Misantla, Mexico, *in* M. E. Gómez-Luna and A. M. Cortez, eds., 5th Latin American Congress of Organic Geochemistry, Cancún, Mexico, Memoir, Abstracts Volume, p. 112–114.

Román-Ramos, J. R., and L. N. Holguín-Quiñones, 2001, Subsistemas generadores de la región norte de Mexico: Boletín Asociación Mexicana de Geólogos Petroleros, v. 49, no. 1–2, p. 68–84.

Seilacher, A., 1967, Bathymetry of trace fossils: Marine Geology, v. 5, p. 413–428.

Trudgill, B. D., M. G. Rowan, J. C. Fiduk, P. Weimer, P. E. Gale, B. E. Korn, R. L. Phair, W. T. Gafford, G. R. Roberts, and S. W. Dobbs, 1999, The Perdido fold belt, northwestern deep Gulf of Mexico: Part 1. Structural geometry, evolution and regional implications: AAPG Bulletin, v. 83, p. 88–113.

Vail, P. R., 1987, Seismic stratigraphy interpretation using sequence stratigraphy: Part I. Seismic stratigraphy interpretation procedure, *in* A. W. Bally, ed., Atlas of

seismic stratigraphy, v. 1: AAPG Studies in Geology 27, p. 1–10.

Van Wagoner, J. C., R. M. Mitchum, K. M. Campion, and V. D. Rahmanian, 1990, Siliciclastic sequence stratigraphy in well logs, cores, and outcrops: AAPG Methods in Exploration Series 7, p. 1–55.

Watkins, J. S., and R. T. Buffler, 1996, Deepwater frontier exploration potential: Gulf Coast Association of Geological Societies Transactions, v. 46, p. 79–94.

Wawrzyniec, T., et al., 2003, Cenozoic deformational styles of the Laguna-Madre–Tuxpan shelf and Mexican Ridges fold belt, Mexico: Gulf Coast Association of Geological Societies Transactions, v. 53, p. 843–854.

Winker, C. D., 1984, Clastic shelf margins of the Post-Comanchean Gulf of Mexico: Implications for deep-water sedimentation, *in* Characteristics of gulf basin deep-water sediments and their exploration potential: Annual Research Conference, Gulf Coast Section SEPM Program and Abstracts, p. 109–120.